Supplementary Information for:

Cell-selective labeling with amino acid precursors for proteomic studies of multicellular environments

Nicholas P Gauthier[1,2], Boumediene Soufi[3], William E Walkowicz[2,4], Virginia A Pedicord[5], Konstantinos J Mavrakis[6], Boris Macek[3], David Y Gin[4,7], Chris Sander[1] & Martin L Miller[1]

[1] Computational Biology Center, Memorial Sloan-Kettering Cancer Center, 1275 York Avenue, New York, New York 10065, USA.
[2] Louis V. Gerstner Jr. Graduate School of Biomedical Sciences, Memorial Sloan-Kettering Cancer Center, 1275 York Avenue, New York, New York 10065, USA.
[3] Proteome Center Tübingen, Auf der Morgenstelle 15, 72076 Tübingen, Germany.
[4] Molecular Pharmacology and Chemistry Program, Memorial Sloan-Kettering Cancer Center, 1275 York Avenue, New York, New York 10065, USA.
[5] Department of Immunology, Memorial Sloan-Kettering Cancer Center, 1275 York Avenue, New York, New York 10065, USA.
[6] Cancer Biology and Genetics Program, Memorial Sloan-Kettering Cancer Center, 1275 York Avenue, New York, New York 10065, USA.
[7] Deceased.
Correspondence should be addressed to N.P.G., C.S., and M.L.M. (ctap@cbio.mskcc.org)

Supplementary Figures **2**
Supplementary Figure 1: Examples of L-lysine producing enzymes and their substrates ... 2
Supplementary Figure 2: Growth of human HEK293T and mouse 3T3 cell lines on L-lysine and different precursors of L-lysine ... 3
Supplementary Figure 3: DDC-expressing HEK293T cells grow specifically on DAP ... 4
Supplementary Figure 4: Precursors have little to no perturbing effect when cells are grown in L-lysine ... 4
Supplementary Figure 5: Precursor- and SILAC-based incorporation reaches steady state after approximately four doublings ... 5
Supplementary Figure 6: Limited mRNA expression differences observed on growth of precursor vs L-lysine ... 6
Supplementary Figure 7: Cells grown on precursors exhibit limited changes in amino acid starvation response factors ... 7
Supplementary Figure 8: Limited protein expression differences observed on growth of precursor vs L-lysine ... 8
Supplementary Figure 9: Growth response to drug perturbation in DAP versus L-lysine and DDC-expressing versus control cells ... 9
Supplementary Figure 10: Molecular response to perturbation in DAP versus L-lysine and DDC-expressing versus control cells ... 9
Supplementary Figure 11: LC-MS/MS depicting differential precursor-based proteome labeling of human-mouse co-culture ... 10
Supplementary Figure 12: LC-MS/MS analysis of labeling between two biological human-mouse co-culture replicates ... 11
Supplementary Figure 13: Sequence optimization of lyr and its impact on label separation in co-culture ... 12
Supplementary Figure 14: Post sort FACS analysis of co-cultured human HEK293T and MDA-MB-231 cells ... 13
Supplementary Figure 15: Label status of differentially labeled co-culture cells shows good agreement with SILAC-labeled monocultures 14
Supplementary Figure 16: Distinguishing the cell-of-origin of secreted proteins in a mixed-species co-culture ... 15
Supplementary Figure 17: Protein label status of co-cultured (CTAP labeled) secretome vs. mono-culture (SILAC labeled) lysates ... 15
Supplementary Figure 18: Cell-selective labeling of co-cultures using one enzyme-precursor pair ... 16
Supplementary Figure 19: Growth and incorporation of Z-lysine in CBZcleaver-expressing 3T3 cells ... 17

Supplementary Tables **18**
Supplementary Table 1: Transgenic cell lines and the precursor-enzyme pairs used for mass spectrometry studies ... 18
Supplementary Table 2: Growth of various cell lines using CTAP enzyme-precursor pairs ... 18
Supplementary Table 3: Incorporation levels of fully labeled cells based on counting light and heavy peaks ... 18
Supplementary Table 4: Changing parameters has little effect on estimated level of label incorporation ... 19
Supplementary Table 5: Gene Set Enrichment Analysis of DDC-expressing 3T3 cells in L-lysine, DAP, or starved conditions ... 20
Supplementary Table 6: Gene Set Enrichment Analysis of lyr-expressing MDA-MB-231 cells in L-lysine, D-lysine, or starved conditions . 21
Supplementary Table 7: Primers and reactions for cloning of lyr ... 22
Supplementary Table 8: Primers and reactions for cloning of DDC ... 23

Supplementary Note 1: Enzyme Sequences **24**
Supplementary Sequence 1: lyr (pLM-MTS-mCherry-lyr$^{\Delta 4\text{-}57nt}$) ... 25
Supplementary Sequence 2: DDC (pLM-GFP-P2A-DDC) ... 26
Supplementary Sequence 3: DDC (MSCV-DDC-IRES-GFP) ... 27
Supplementary Sequence 4: CBZcleaver (MSCV-CBZcleaver-IRES-mCherry) ... 28
Supplementary Sequence 5: Wild-type lyr (pLM-mCherry-P2A-Wild-type lyr) ... 29

Supplementary Note 2: Synthesis of Z-lysine [N^{α}-Cbz-L-lysine(K8)] **30**

Supplementary Discussion **31**

Bibliography **32**

Supplementary Figures

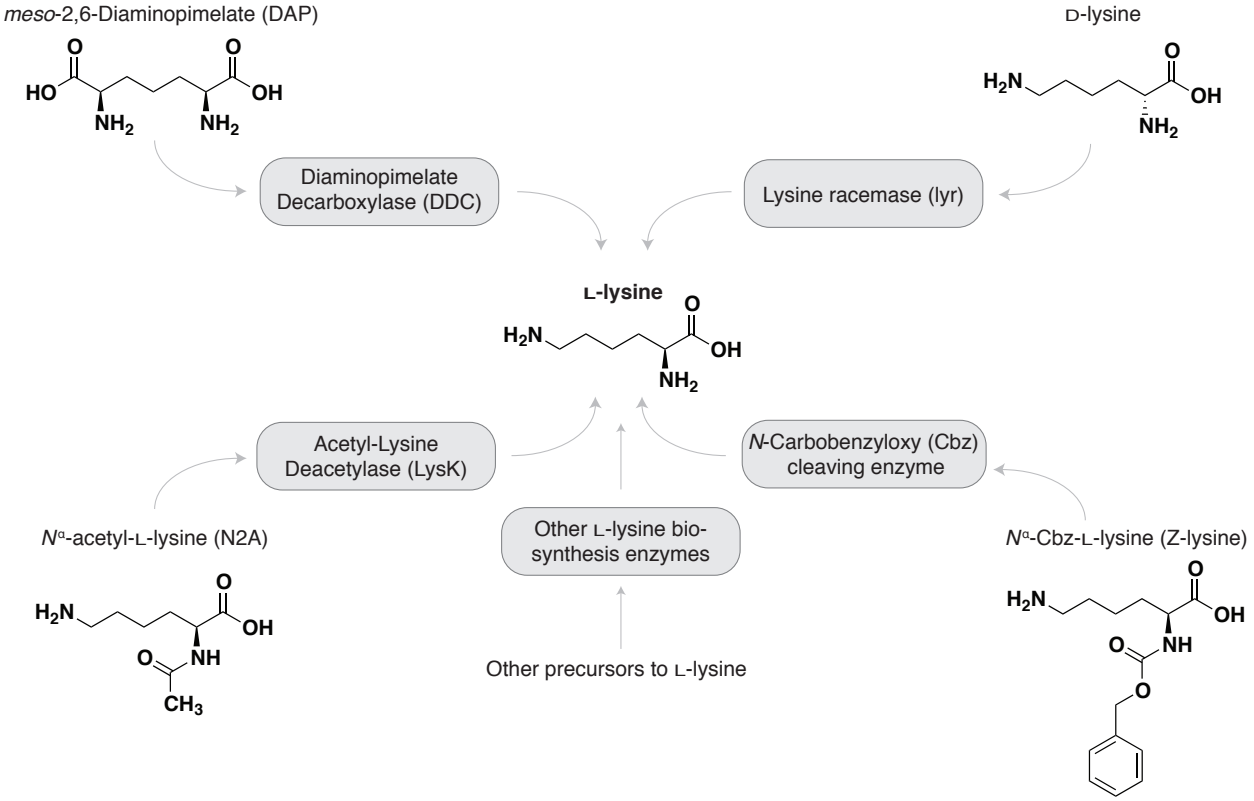

Supplementary Figure 1: **Examples of L-lysine producing enzymes and their substrates.** Several enzymes have been found in bacteria, fungi, and plants that catalyze reactions leading to the production of L-lysine from precursor compounds. Four examples of these enzymes and their respective precursors are indicated. Note that while the substrate of DDC is only the *meso*- form DAP, in this work the DAP used contains DD-, LL-, and the *meso*- form.

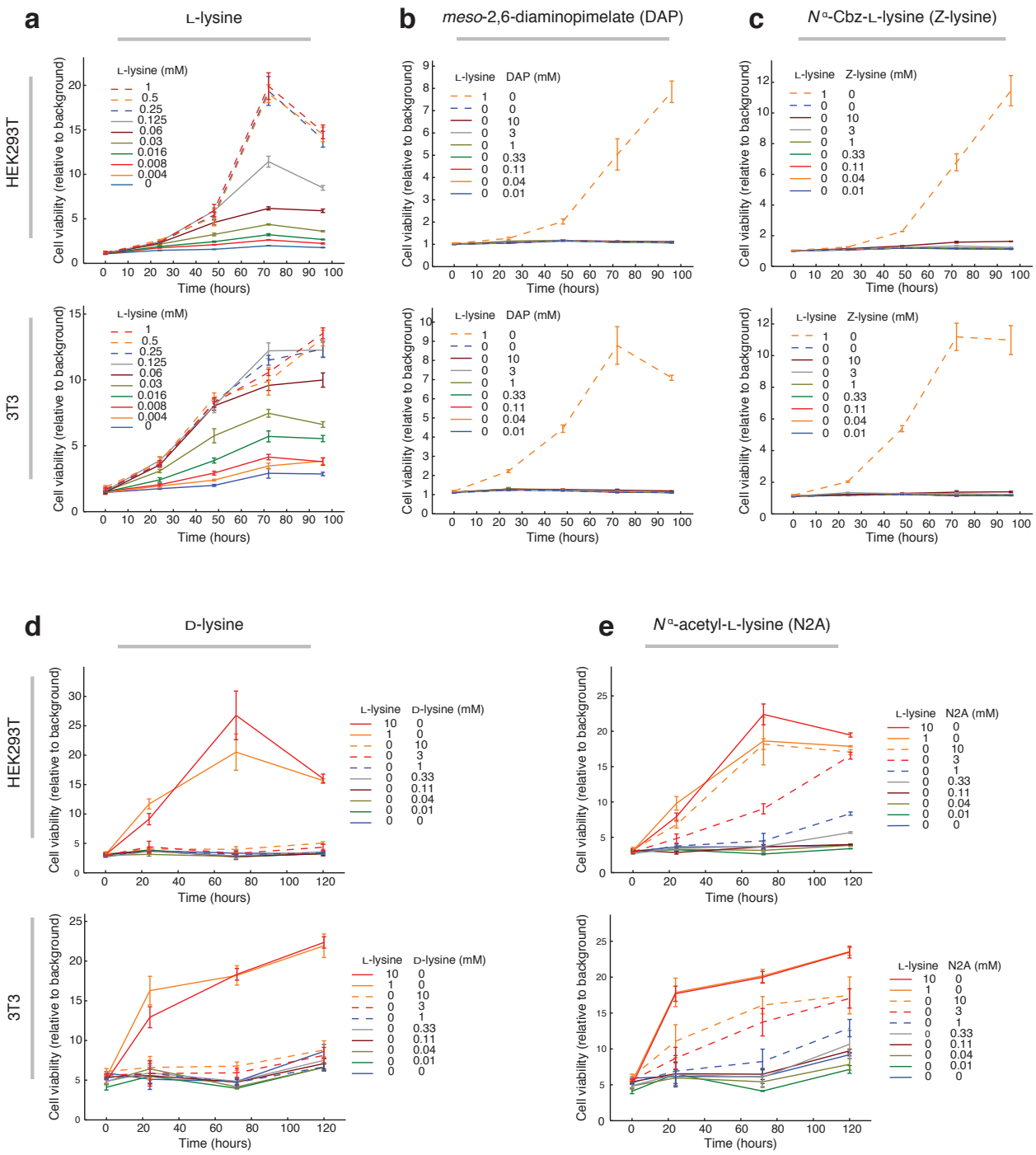

Supplementary Figure 2: **Growth of human HEK293T and mouse 3T3 cell lines on L-lysine and different precursors of L-lysine.** (**a**) Cells were seeded in 96-well format and cell proliferation was measured with the Resazurin (AlamarBlue) assay at the time indicated. Note that both cell lines stop growing when no L-lysine is present, confirming that mammalian cells are L-lysine auxotrophic. Cells show no or limited growth response when the medium is supplemented with high (mM-range) concentrations of the L-lysine precursors 2,6-diaminopimelic acid (DAP, **b**), N^{α}-Cbz-L-lysine (Z-lysine, **c**), and D-lysine (**d**). In contrast, both cell lines grow when the medium is supplemented with high concentrations of N^{α}-acetyl-L-lysine (N2A, **e**). Errors bars represent the standard deviation of at least four replicates per condition.

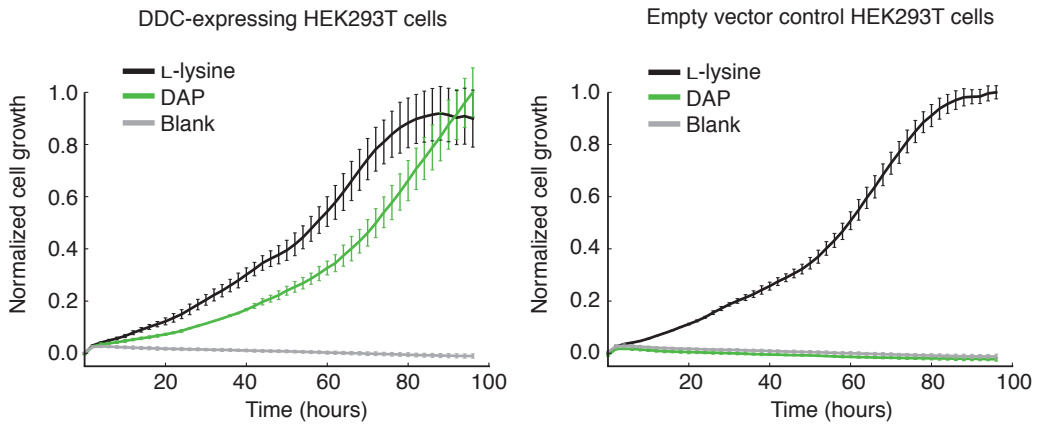

Supplementary Figure 3: **HEK293T cells expressing the L-lysine biosynthesis enzyme diaminopimelate decarboxylase (DDC) specifically grow on 2,6-diaminopimelic acid (DAP).** HEK293T cells stably transfected with DDC (left panel) or empty control vector (right panel) were cultured in 0.798 mM L-lysine, 10 mM DAP, or neither (blank). Cell growth was estimated by the impedance-based xCELLigence assay and data was normalized to the maximum value for each cell-type. Note that only HEK293T cells that express DDC grow on DAP. Error bars represent the standard deviation of three replicates per condition.

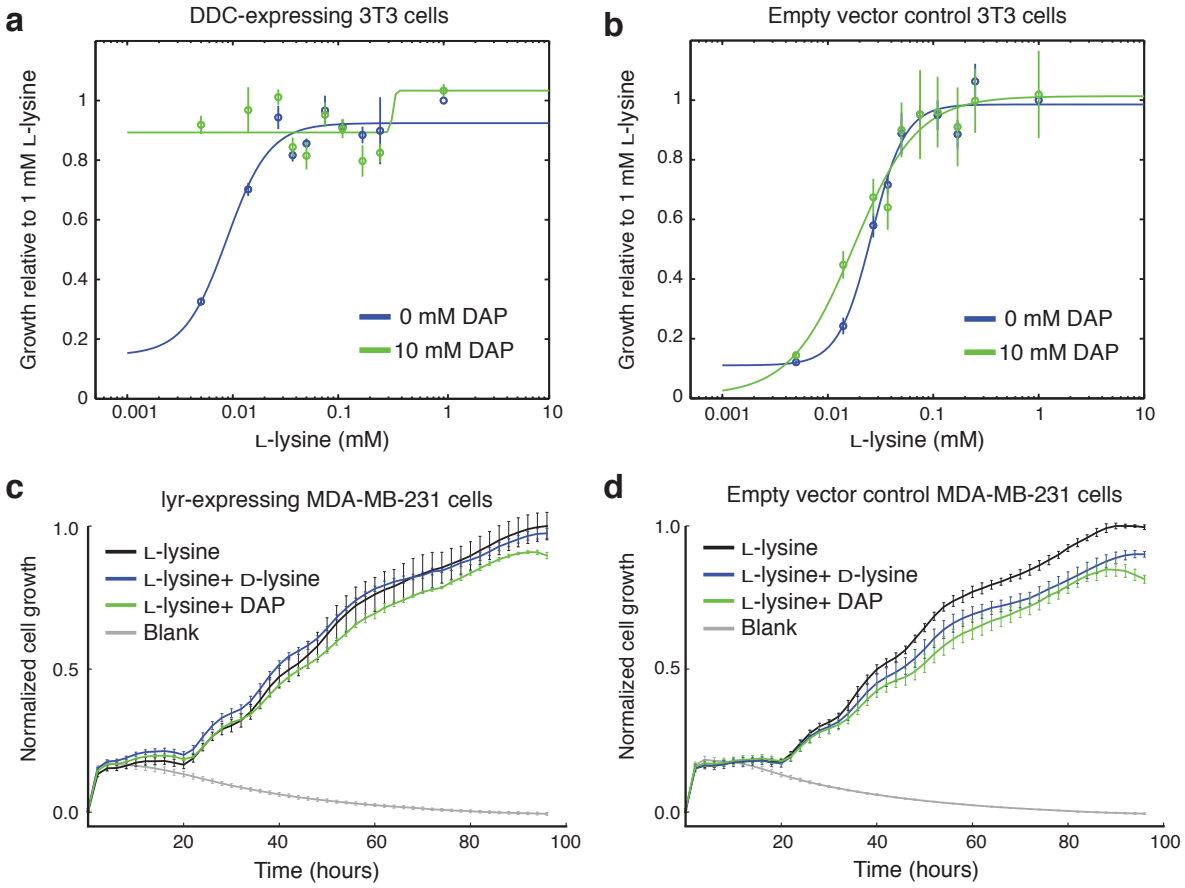

Supplementary Figure 4: **Precursors have little to no perturbing effect when cells are grown in L-lysine.** (**a**) 3T3 cells expressing DDC or (**b**) empty vector control were plated in different concentrations of L-lysine with or without 10 mM DAP. After three days, cell growth was estimated by the Resazurin assay. MDA-MB-231 cells expressing (**c**) lyr and (**d**) empty vector control were plated in 0.798 mM L-lysine or L-lysine combined with 4 mM D-lysine or 10 mM DAP. Cell growth was determined with xCelligence periodically for four days. The mean and standard deviation of least three replicates are shown.

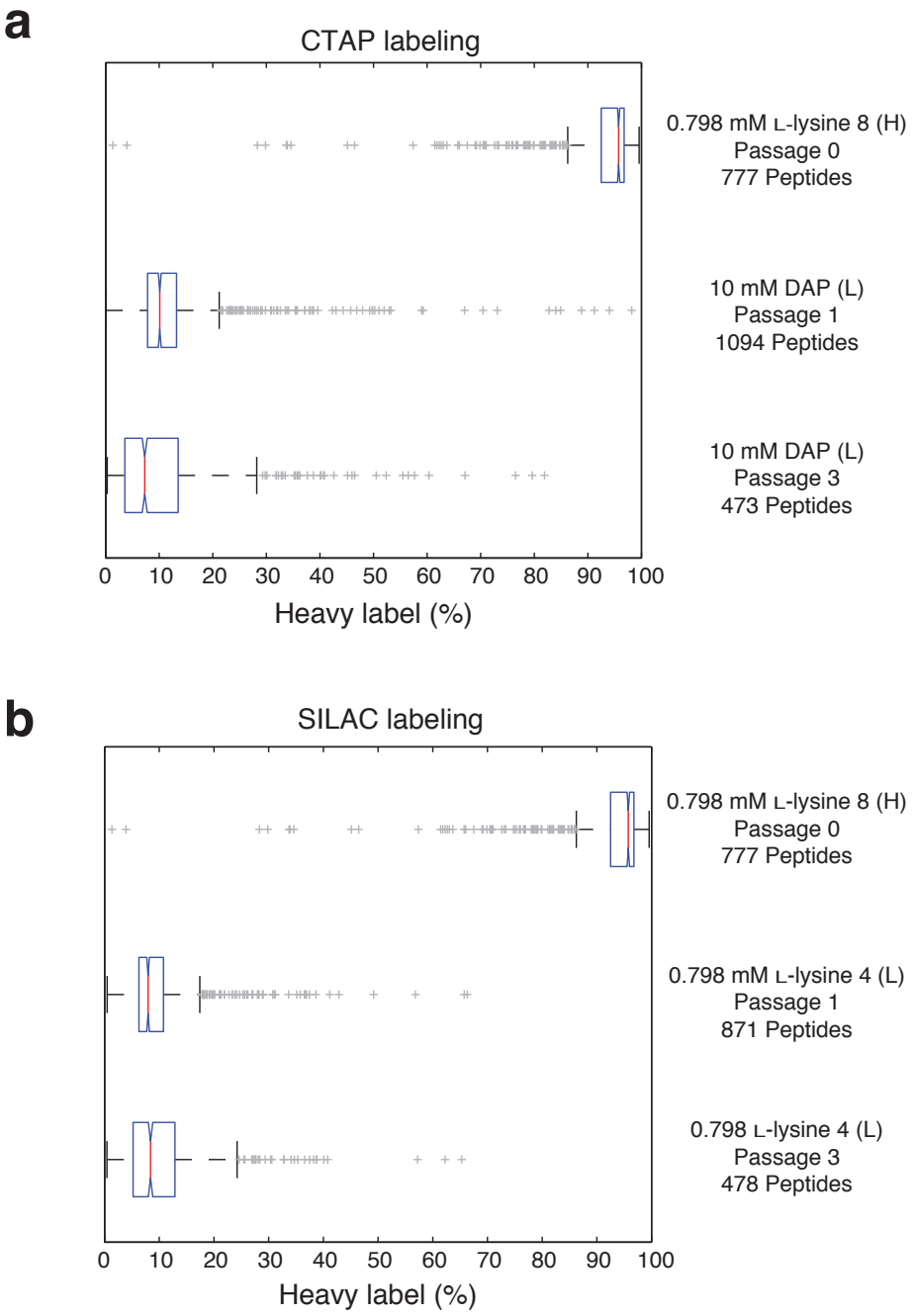

Supplementary Figure 5: **Precursor-based and SILAC-based incorporation reaches steady state after approximately four doublings.** DDC-expressing 3T3 cells were prelabeled with heavy L-lysine and were passaged three times in either (**a**) light labeled DAP or (**b**) medium labeled L-lysine. Cells doubled approximately four times per passage. Samples prepared at the start of the experiment, passage one, and passage three, were subjected to LC-MS/MS. Each box represent one sample. The center red line is the median observation, the edges of the box are the 25th and 75th percentiles, and the whiskers extend to the most extreme values not considered outliers.

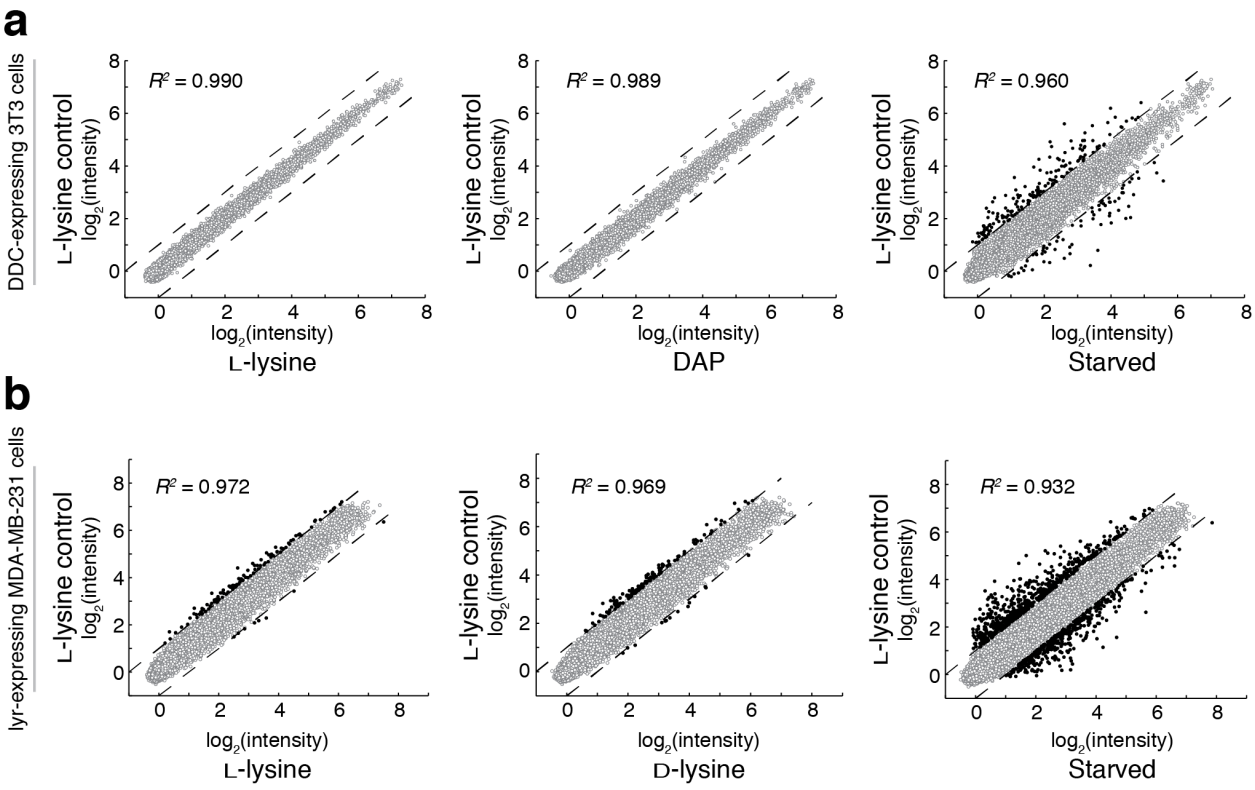

Supplementary Figure 6: **Limited mRNA expression differences observed on growth of precursor vs L-lysine.** (**a**) 3T3 cells expressing DDC were plated on L-lysine, DAP, or in DAP/L-lysine free (starved) conditions. After 72 hours, mRNA was harvested and run on the Illumina microarray platform. Representative arrays of three biological replicates are shown. Black dots represent genes that change more than two-fold between conditions. Dashed lines depict boundaries for 2-fold expression ratios between samples. (**b**) Similar to (**a**) except MDA-MB-231 cells expressing lyr were plated on L-lysine, D-lysine, or in starved conditions.

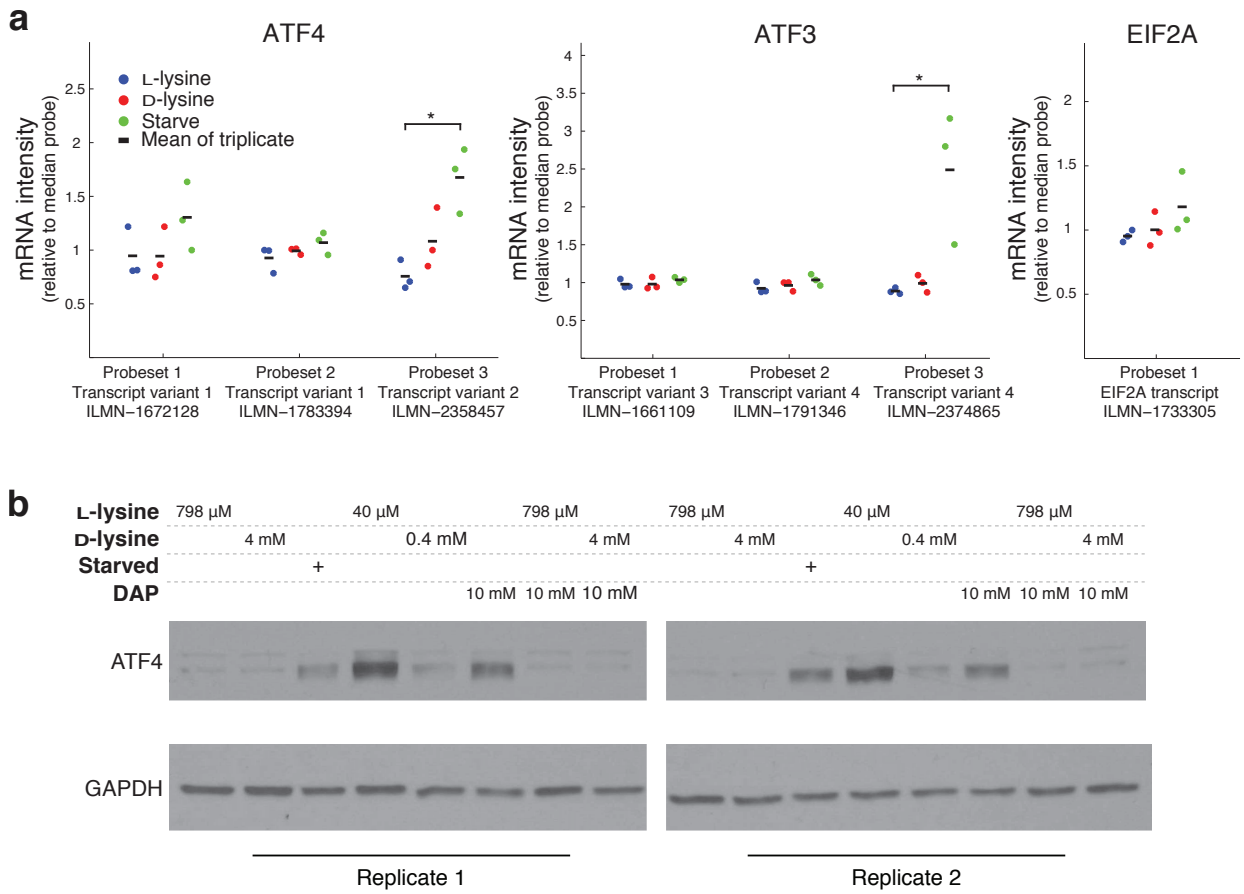

Supplementary Figure 7: **Cells grown on precursors exhibit limited changes in amino acid starvation response factors.** (**a**) Individual probes of the amino acid starvation response factors (ATF4, ATF3, and EIF2A) were analyzed using gene expression data obtained from the microarray-based profiling of lyr-expressing MDA-MB-231 cells (see **Fig. 3b** & **Supplementary Fig. 6b**). Each dot represents the intensity in a single sample relative to the median intensity across all samples of the indicated probe. Two-sample, two-tailed student's t-tests were used to compare the L-lysine condition to either the D-lysine or the starved condition and an asterisk indicates a significance level below 0.05. (**b**) Lyr-expressing MDA-MB-231 cells were cultured for three days in SILAC media supplemented with L-lysine, precursors (D-lysine or DAP), or without either (starved). Cells were lysed and the level of ATF4 was assessed by western blot. Note that the level of ATF4 is low in 0.798 mM L-lysine and 4 mM D-lysine. For negative controls, cells were cultured without L- or D-lysine (starved), in lower concentrations of either molecule (40 µM L-lysine or 400 µM D-lysine), or in the presence of DAP alone, resulting in an an upregulation of ATF4. Unexpectedly, ATF4 expression appears slightly higher in the low levels of L-lysine (40 µM) than in the starved condition. Protein loading is indicated with GAPDH.

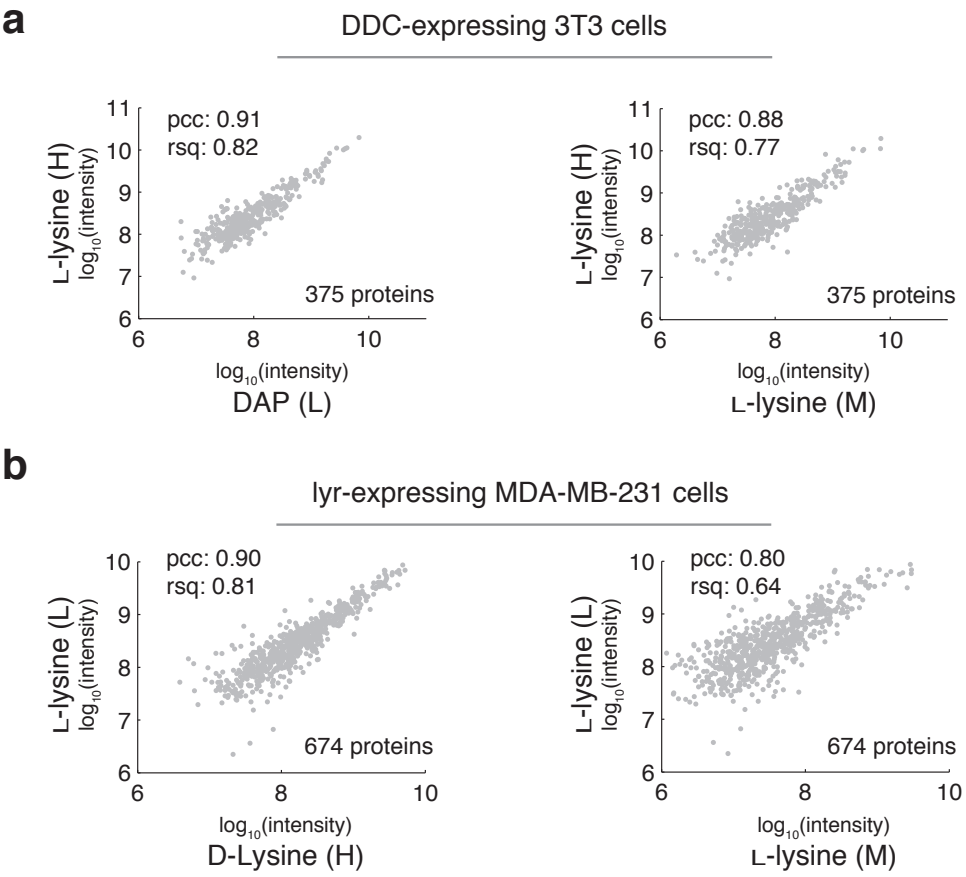

Supplementary Figure 8: **Cells grown on precursors exhibit few or no protein abundance changes relative to those grown on L-lysine.** (**a**) DDC-expressing 3T3 cells were grown on either 10 mM DAP, 0.798 mM medium L-lysine (M), or 0.798 mM heavy L-lysine (H), and were analyzed by LC-MS/MS. Using the MaxQuant software, the protein intensities were compared between the conditions. Pearson correlation coefficients (pcc) and r-squared values (rsq) are provided. (**b**) Similar to (**a**) except lyr-expressing MDA-MB-231 were grown on 4 mM heavy D-lysine (H), light 0.798 mM L-lysine (L), or 0.798 mM medium L-lysine (M). Note that the correlation between cells grown on precursor versus L-lysine (left panels) is similar to that of cells grown on two different stable isotopes of L-lysine (SILAC-labeled biological replicate, right panels). Each condition represents one sample processed by LC-MS/MS and the number of common proteins is indicated.

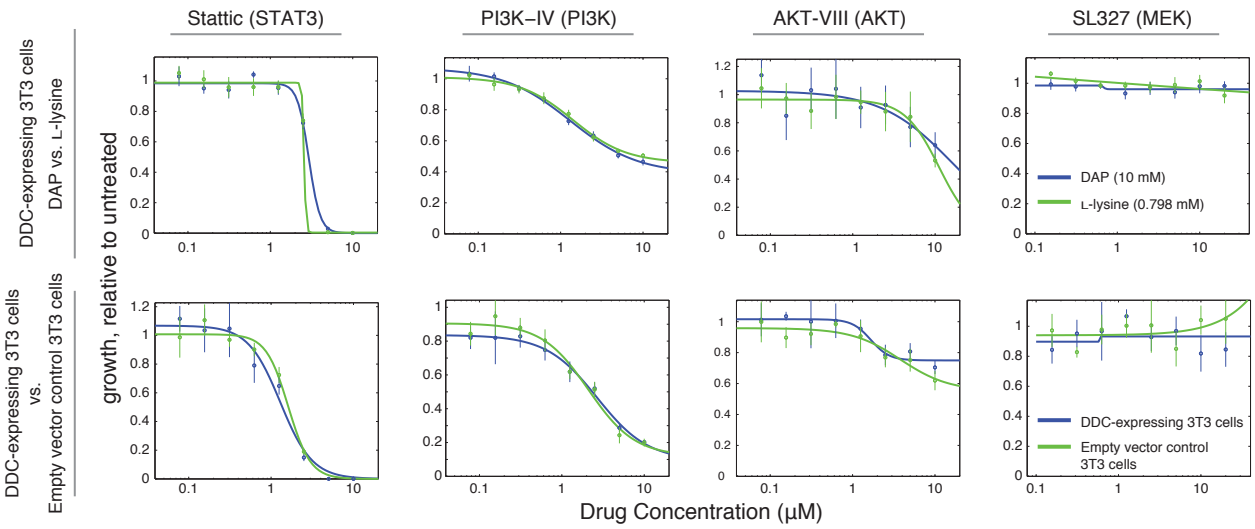

Supplementary Figure 9: **Drug perturbation induces comparable effects to cell viability for both cells on DAP versus L-lysine and enzyme-expressing versus empty-vector control cells.** In the upper panel, DDC-expressing 3T3 cells were grown in the presence of either 10 mM DAP (green) or 0.798 mM L-lysine (blue) in various concentrations of drugs as indicated (target of drug is indicated in parenthesis). Cell viability was measured after 48 hours of drug exposure with the Resazurin assay and normalized to untreated control cells. The lower panel compares DDC-expressing 3T3 cells (green) to empty vector control cells (blue) in the presence of 0.798 mM L-lysine. Errors bars represent the standard deviation of at least four replicates per condition.

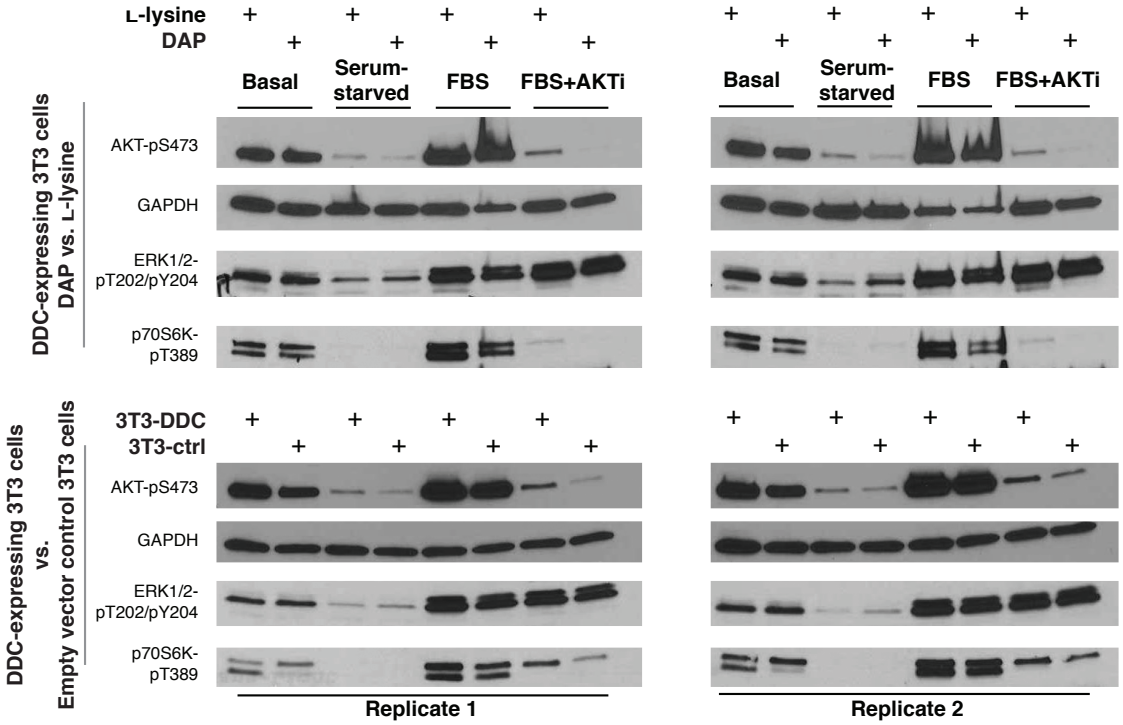

Supplementary Figure 10: **Molecular response to starvation, FBS stimulation, and drug perturbation are largely similar for both cells on DAP versus L-lysine as well as enzyme-expressing versus empty-vector control cells.** In the upper panel, DDC-expressing 3T3 cells were grown in the presence of either 10 mM DAP or 0.798 mM L-lysine in media with 10% FBS (basal), without FBS (serum-starved), starved for 24h and stimulated with 10% FBS for 1h (FBS), or stimulated with FBS and perturbed with 5 μM AKT Inhibitor VIII (EMD Chemicals) for 1h (FBS+AKTi). In the lower panel, DDC-expressing 3T3 cells (3T3-DDC) and empty vector control cells (3T3-ctrl) were grown in the presence of 0.798 mM L-lysine and exposed to similar conditions. For both experiments, cells were lysed and the response of several phosphoproteins was assessed by western blotting. Loading is indicated with GAPDH. Two biological replicates are shown. For western blot protocol, see **Supplementary Methods**.

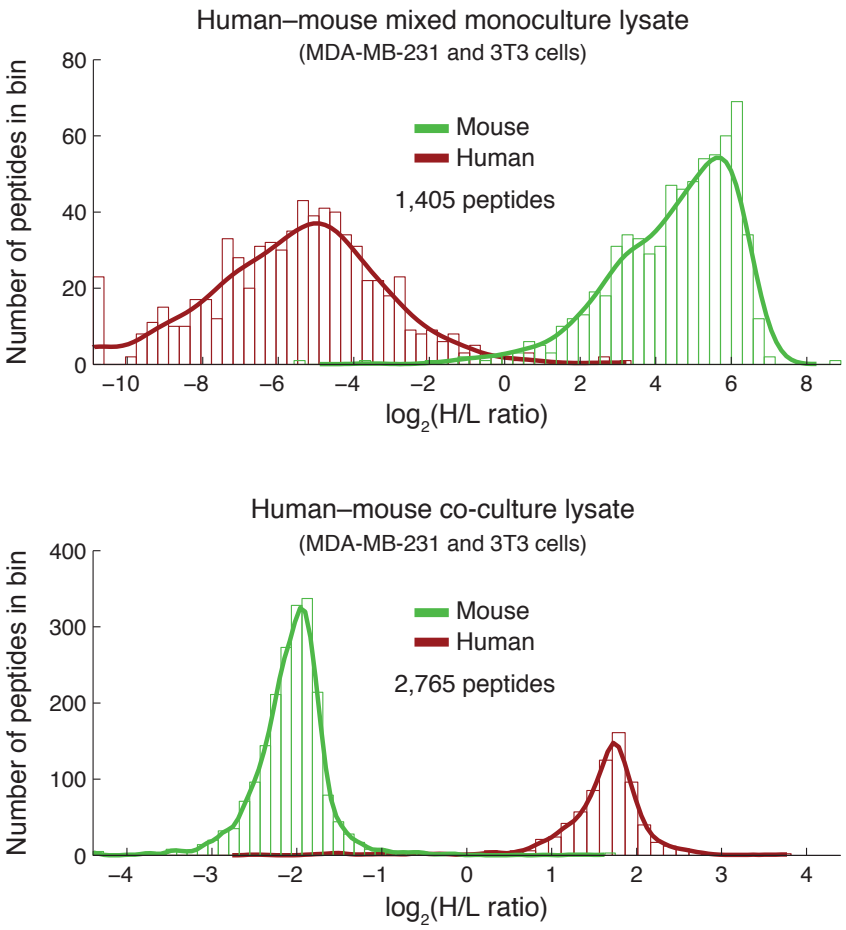

Supplementary Figure 11: **Using two distinct enzyme-precursor pairs, co-cultured cells exhibit precursor-based differential proteome labeling.** DDC-expressing 3T3 cells (mouse) were labeled with heavy L-lysine (H) and lyr-expressing MDA-MB-231 cells (human) with light L-lysine (L) and mixed prior to sample analysis by LC-MS/MS (upper panel). Similarly labeled cells were co-cultured and analyzed after 10 days (two passages) on DAP (L) and D-lysine (H) (lower panel). Peptides unique to the mouse or human proteome are green and red, respectively. For each histogram, 50 bins were used and a nonparametric kernel-smoothing function was applied to fit the distribution. Each panel depicts one sample processed by LC-MS/MS. Note that the data presented here is similar to depicted in **Fig. 4a**.

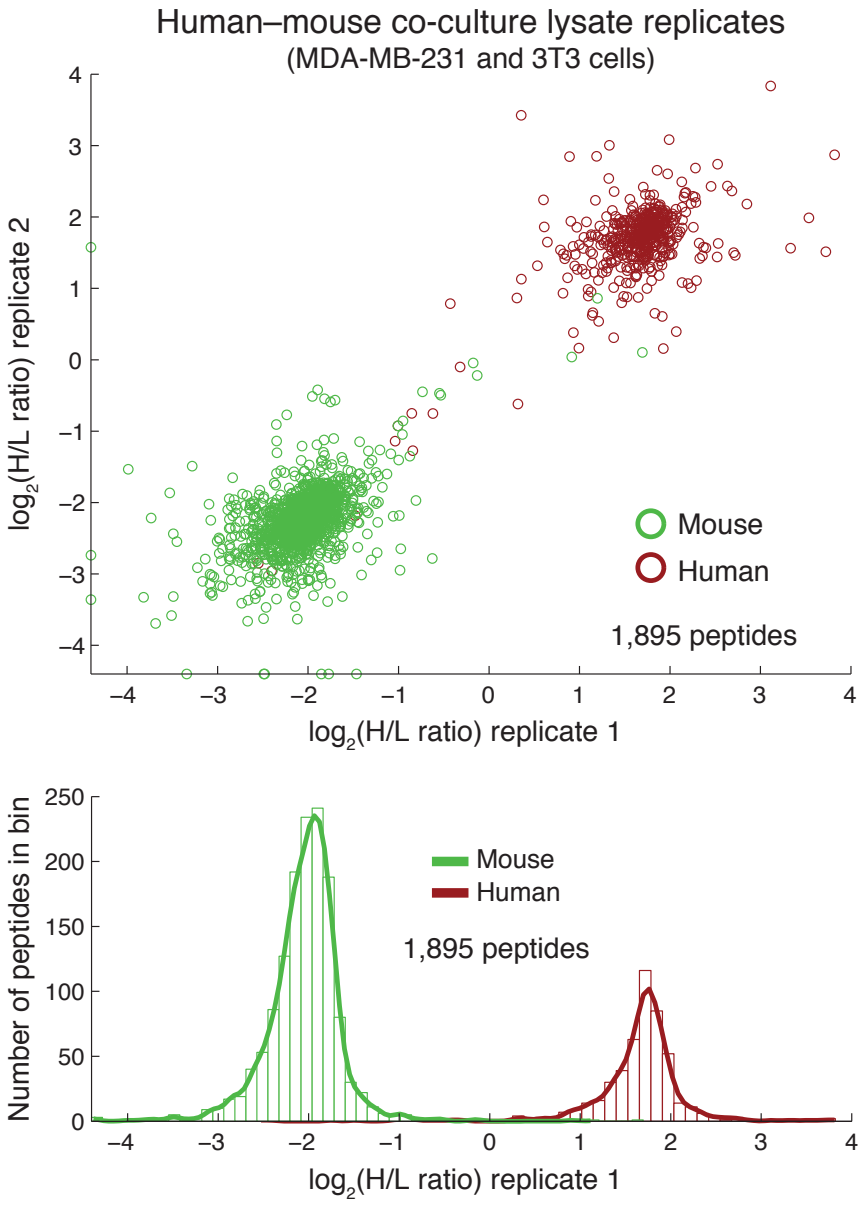

Supplementary Figure 12: **Analysis of H/L ratios of species-specific peptides identified across two biological replicates of a human and mouse co-culture.** DDC-expressing 3T3 cells (mouse) and lyr-expressing MDA-MB-231 cells (human) were cultured for 10 days (two passages) on DAP (L) and D-lysine (H) in L-lysine-free conditions. The co-cultures were lysed and processed for LC-MS/MS analysis. Two biological replicates of H/L ratios of human (red) and mouse (green) specific peptides are shown. The lower panel displays the same data using histograms with 50 bins each.

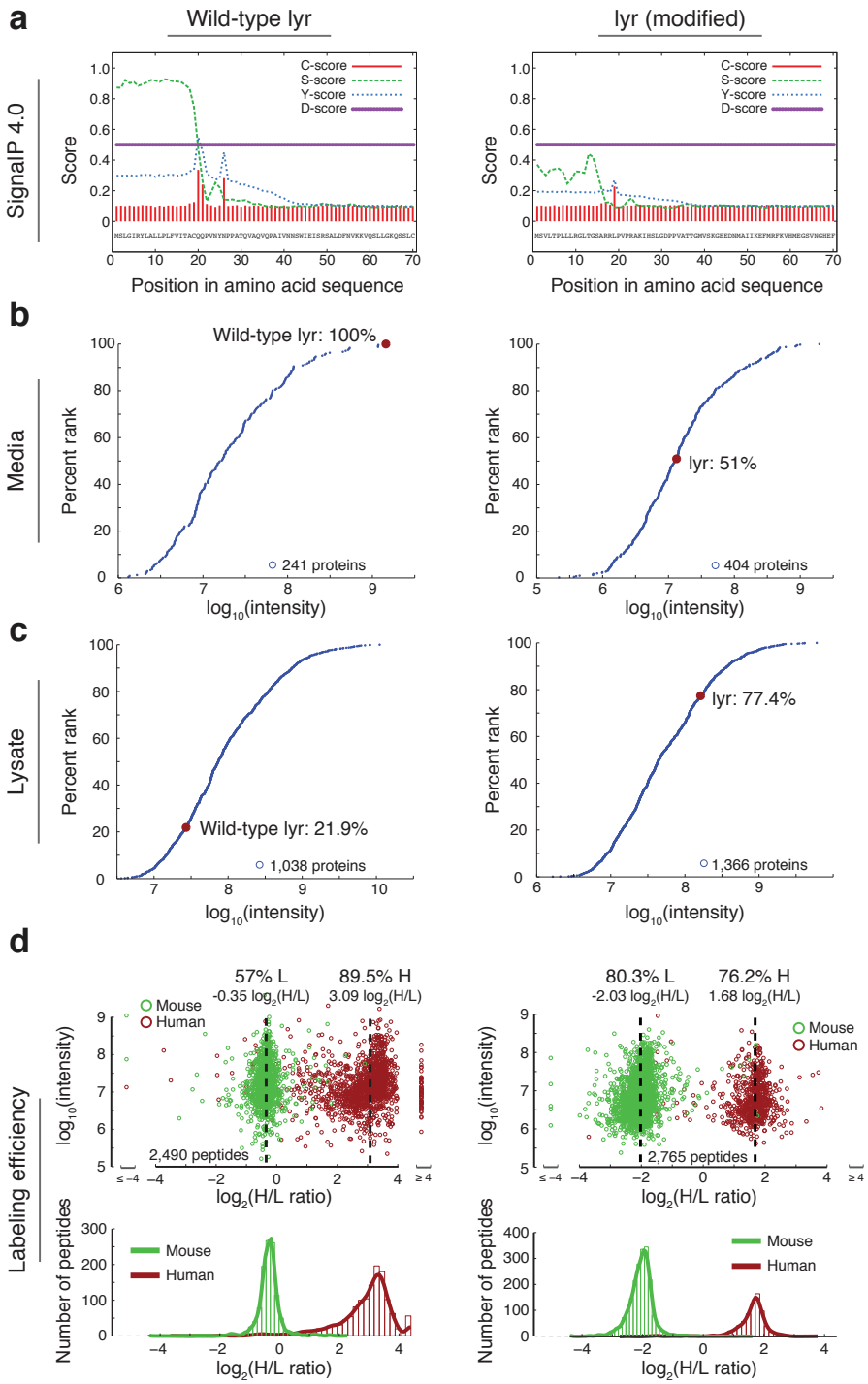

Supplementary Figure 13: **Sequence modification of lyr suppresses signal peptide prediction score, reduces amount of extracellular lyr, and improves label separation in CTAP-labeled co-cultures.** (**a**) Artificial neural network score using SignalP 4.0 of amino acid sequences from full length lyr (wild-type lyr, left) and lyr with 18 amino acids removed from the N-terminus and fused to mCherry containing a mitochondrial targeting signal (modified lyr, right). See **Supplementary Sequences** for schematics of each construct. Default settings in SignalP were applied using the eukaryotic prediction mode. C-score: raw cleavage site score; S-score: signal peptide score; Y-score: combined cleavage site score. Note that only wild-type lyr has a positive predicted signal peptide as the combined Y-score (dotted blue line) exceeds the discrimination score of 0.5 (D-score, purple line) at amino acid number 20. (**b**) Intensity ranked proteins identified by MS in the media of DDC-expressing HEK293T cells co-cultured with MDA-MB-231 cells that express either wild-type lyr (left) or modified lyr (right). Note that while wild-type lyr is the most intense of all identified proteins in the media, the intensity of modified lyr in the media is decreased to the 51st percentile. (**c**) Similar to (**b**) but samples were prepared directly from cell lysate rather than from cultured media. Note that the reciprocal trend was observed in the cellular lysate. (**d**) DDC-expressing 3T3 cells (mouse) and lyr-expressing MDA-MB-231 cells (human) were cultured for three passages (13 days, left) or two passages (10 days, right) on DAP (L) and D-lysine (H) in L-lysine-free conditions. The co-cultures were lysed and processed for LC-MS/MS analysis. H/L ratios of human (red) and mouse (green) specific peptides from one sample are shown. The lower panel displays the same data using histograms with 50 bins each.

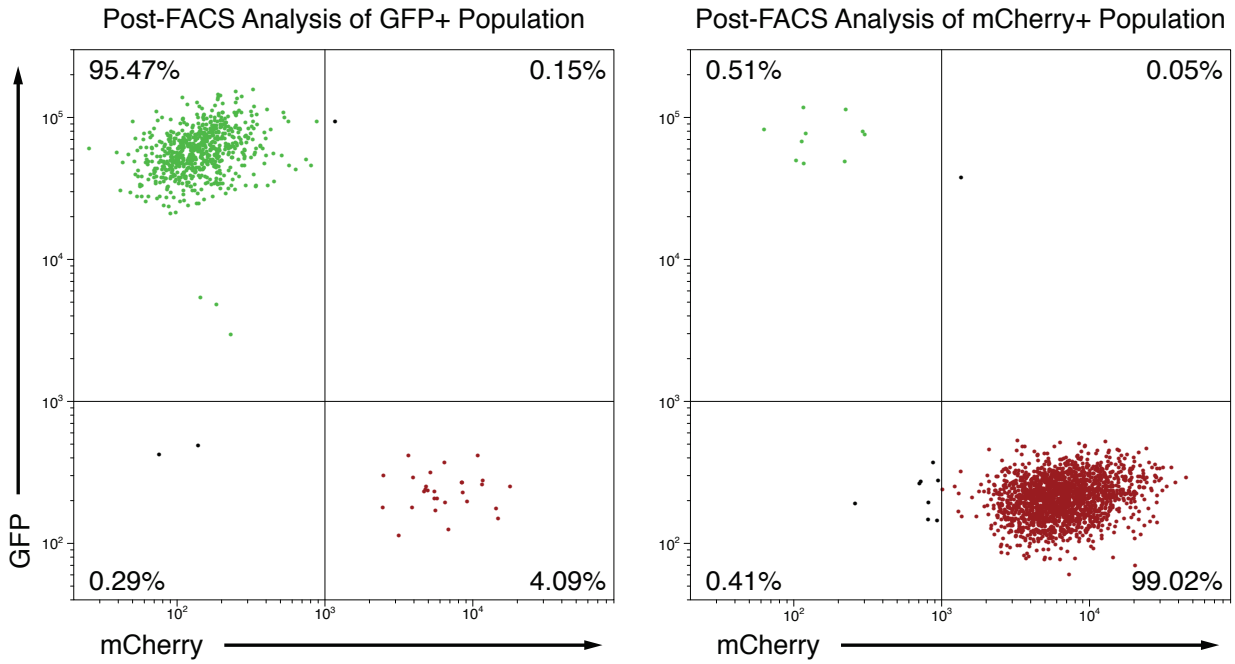

Supplementary Figure 14: **Post sort FACS analysis of co-cultured human HEK293T and MDA-MB-231 cells.** GFP+ HEK293T expressing DDC were co-cultured with mCherry+ MDA-MB-231 cells expressing lyr and sorted for GFP+ and mCherry+ cells by FACS. Depicted is a post-sort analysis showing the purity of each of the sorted populations as assessed by flow cytometry. Percentages are indicated. Although a post-sort analysis of the sorted populations showed a high enrichment for the expected fluorophores, there was small amount of cross-contamination.

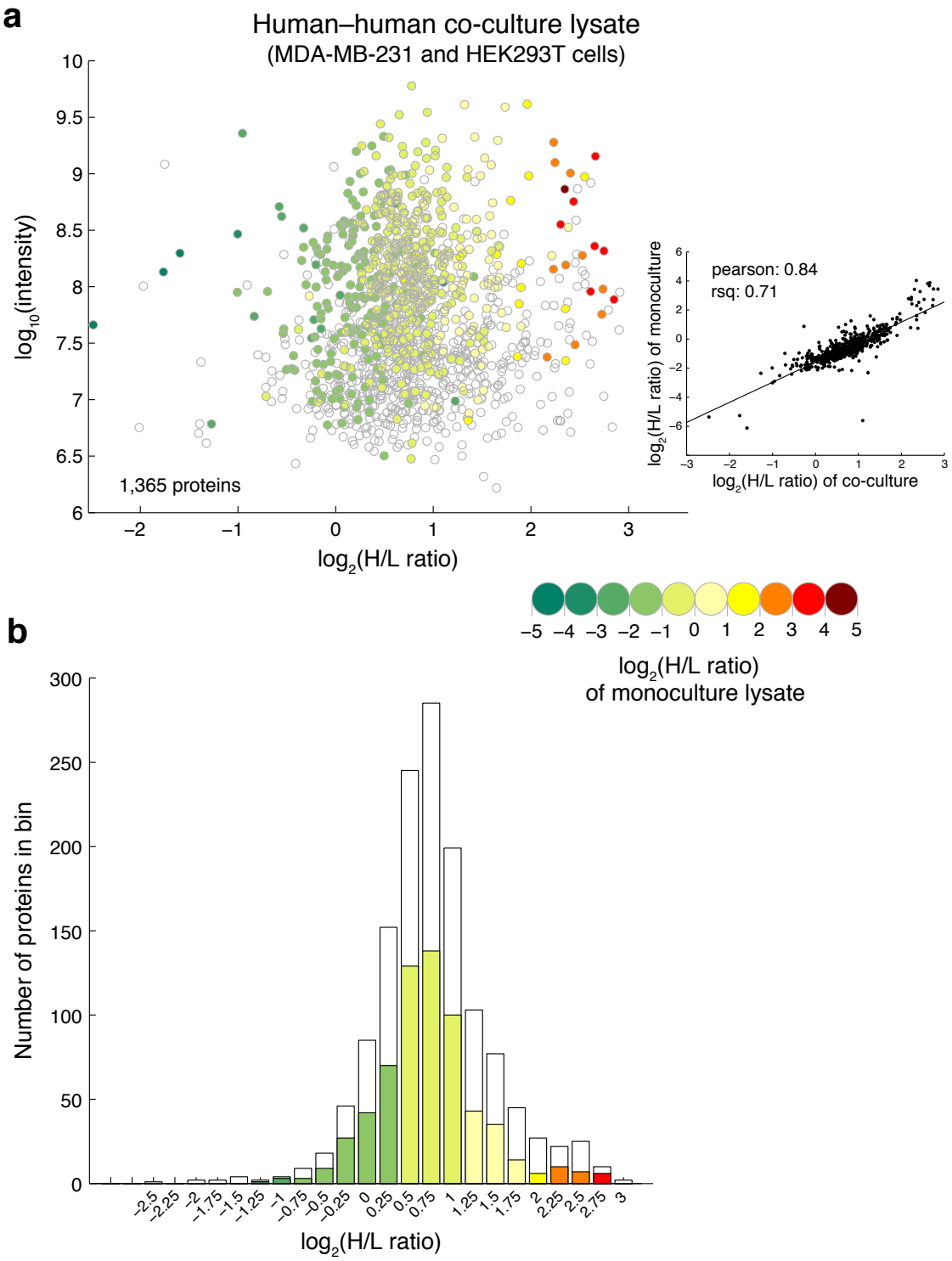

Supplementary Figure 15: **Label status of differentially labeled co-culture cells shows good agreement with SILAC-labeled monocultures.** (**a**) HEK293T expressing DDC cells were co-cultured with MDA-MB-231 cells expressing lyr in 10 mM DAP (L) and 1 mM D-lysine (H). Cell lysate was collected, proteins were digested, and the sample was subjected to LC-MS/MS. Colors depict relative protein abundance as determined by quantitation (median-centered H/L ratios) of mixed mono-cultures that were separately labeled using standard SILAC labeling. Uncolored points represent proteins that were not identified in the mono-culture sample. Inset depicts correlation between mono- and co-culture H/L ratios. (**b**) Co-culture H/L ratios were binned and the average mono-culture H/L ratio in each bin was determined and depicted using a similar color scheme as in (**a**). Each plot compares a single mono- and co-culture sample.

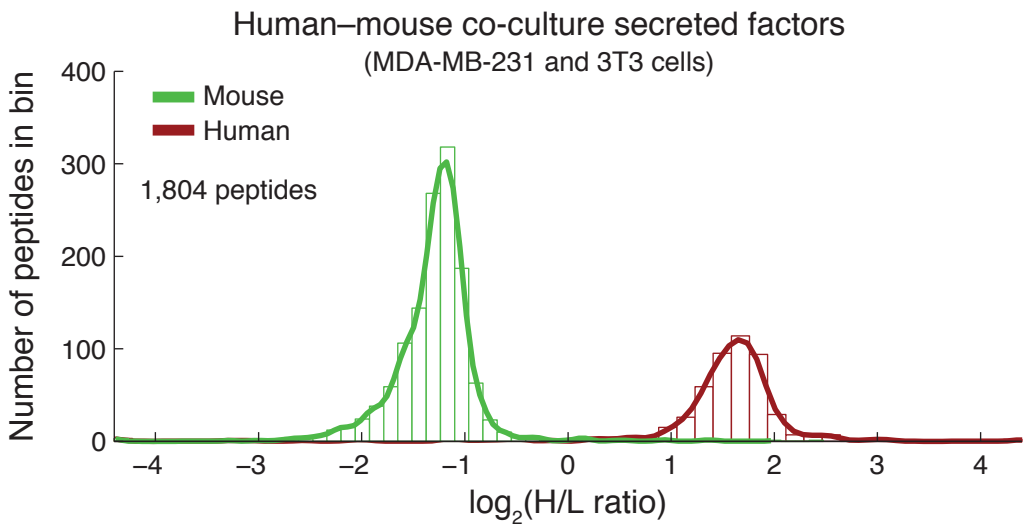

Supplementary Figure 16: **Distinguishing the cell-of-origin of secreted proteins in a mixed-species co-culture.** DDC-expressing 3T3 cells (mouse) and lyr-expressing MDA-MB-231 cells (human) were co-cultured in DAP (L) and D-lysine (H). Prior to sample collection, cells were grown for 16 hours in serum-free medium and the supernatant (medium) was collected. After concentrating proteins by ultra-centrifugation and methanol-chloroform extraction, the sample was analyzed by LC-MS/MS. Only peptides that are unique to mouse (green) and human (red) are displayed. One sample processed by LC-MS/MS is depicted. Note that the data presented here is similar to depicted in **Fig. 5a**.

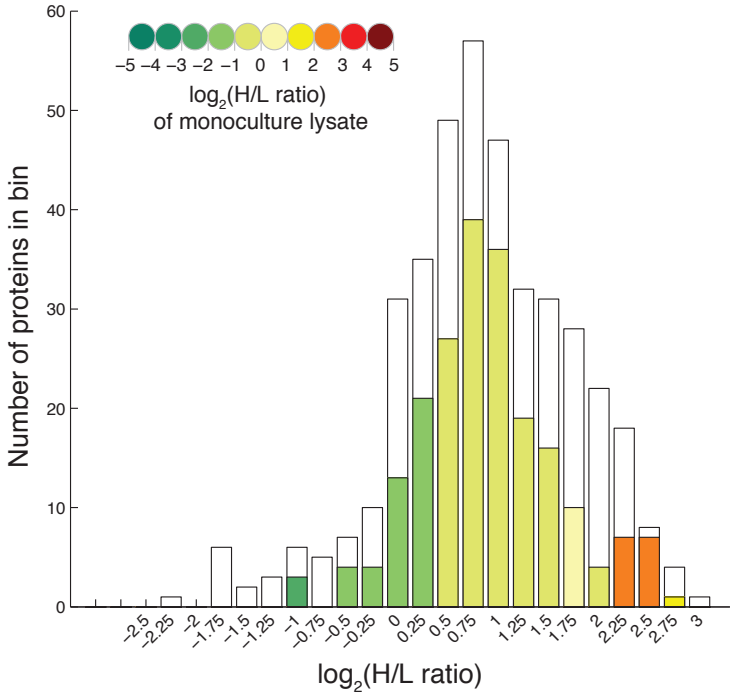

Supplementary Figure 17: **Label status of secreted proteins from differentially labeled co-culture cells shows good agreement with SILAC-labeled mono-culture lysate.** HEK293T expressing DDC cells were co-cultured with MDA-MB-231 cells expressing lyr in 10 mM DAP (L) and 1 mM D-lysine (H). Prior to harvest of supernatant (24 h), cells were grown in serum-free medium. Proteins were concentrated by ultra-centrifugation, precipitated by methanol-chloroform, digested, and subjected to LC-MS/MS. To investigate if the H/L ratios reflect the relative protein abundance between each cell-type, we analyzed whether monoculture intracellular protein levels correlate with those found extracellularly. To test this, the quantified H/L ratios of the secreted proteins were compared to median-centered H/L ratios from mixed mono-cultures that were separately labeled using standard SILAC procedures. The histogram depicts binned H/L ratios from the secreted proteins of a single sample, with the color set to the average mono-culture H/L ratio (one sample) for that bin. Note that a relatively high proportion of the proteins identified with high H/L ratios could not be identified intracellularly (uncolored portion of bars).

Differential proteome labeling of co-cultures using one enzyme-precursor pair

In certain co-culture models, it may be desirable or necessary to use CTAP for labeling a single cell type of interest utilizing only one enzyme-precursor pair. In such a situation, supplementing L-lysine is necessary to allow for growth of the wild-type cells, but creates competition between L-lysine and precursor-based L-lysine for the cell-type of interest. To investigate the balance between precursor- and L-lysine-based growth, we plated GFP+ DDC-expressing 3T3 cells cells together with control 3T3 mCherry+ cells in the presence and absence of DAP. Various concentrations of L-lysine were added to the media and the number of GFP+ and mCherry+ cells were measured by flow cytometry after three days in co-culture. In our assays, the presence of DAP allowed the DDC-expressing cells to outgrow control cells in low levels of L-lysine. In the absence of DAP, both DDC-expressing and control cells exhibited similar growth rates at all L-lysine concentrations tested (**Supplementary Fig. 18a**). At approximately 40 μM L-lysine allowed for growth of both cell types as well as precursor-based growth of the cell-type of interest.

We next used mass spectrometry analysis to test if the cell-type of interest could be selectively labeled in this co-culture setup. At the start of the experiment, heavy L-lysine (H) labeled DDC-expressing mouse 3T3 cells were mixed with medium L-lysine (M) labeled human MDA-MB-231 cells and plated in media supplemented with 40 μM heavy L-lysine (H) and light 10 mM DAP (L). Using two sets of peptides unique to either human or mouse and focusing on the 200 most intense peptides from each set, the expected labels of human-specific and mouse-specific peptides at the start of the experiment were confirmed to be primarily medium and heavy, respectively (**Supplementary Fig. 18b**). After eight days (two passages), the human cells fully exchanged their proteome and became heavy labeled, while the mouse proteome was labeled by both light and heavy. The percentage of light label was significantly increased only in the mouse-specific peptides (from 5% to 23%, $P < 5.6e\text{-}34$, two-tailed students t-test), while the human-specific light label remained unchanged (from 7% to 8%, $P < 0.31$). As expected, full precursor-based labeling was not obtained, likely due to supplementation of L-lysine to the co-culture media. The shift from isotopically-labeled heavy L-lysine (H) to precursor-based light L-lysine (L), which is observed only in enzyme-expressing mouse cells, demonstrates cell-selective labeling in co-culture using a single enzyme-precursor pair. These findings are potentially relevant for identifying biomarkers originating from a cell-type of interest in the context of its natural multicellular environment.

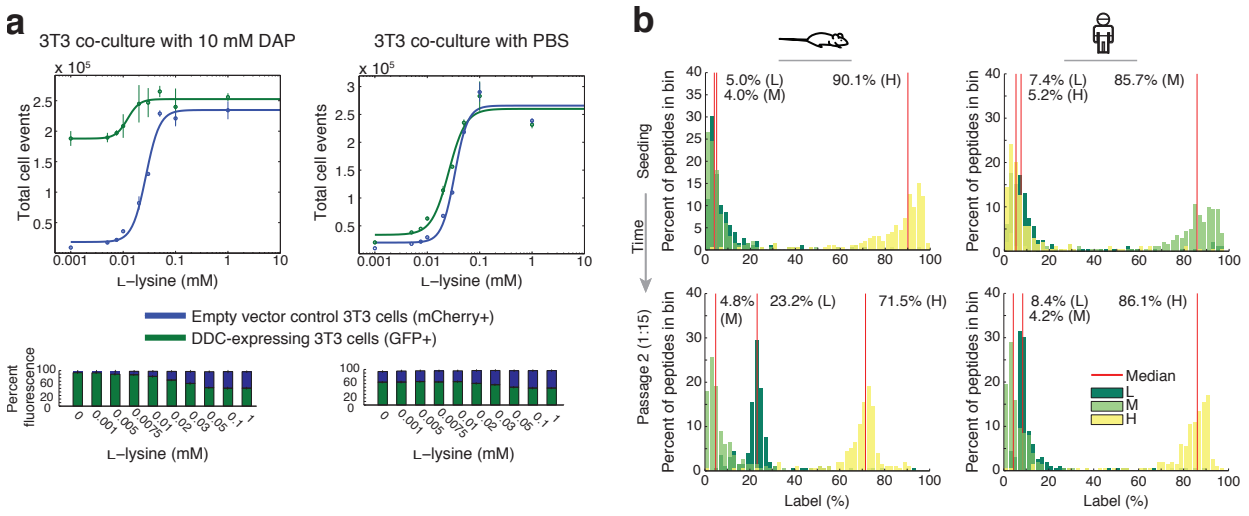

Supplementary Figure 18: **Cell-selective labeling of co-cultures using one enzyme-precursor pair.** (**a**) Co-culture of DDC expressing GFP+ 3T3 cells and empty vector control mCherry+ 3T3 cells with (left panel) or without (right panel) 10 mM DAP and various concentrations of L-lysine. After 72 h in co-culture, flow cytometry was used to determine the number of GFP+ and mCherry+ cells. Error bars represent the standard deviation of at least two biological replicates. (**b**) Mouse 3T3 cells expressing DDC were labeled with heavy L-lysine (H) and human wild-type MDA-MB-231 cells were labeled with medium L-lysine (M). Cell lysates from these separately labeled cells were combined, analyzed by LC-MS/MS, and labeling status of peptides unique to the mouse (top panel, left) and human (top panel, right) proteome were determined. Co-cultures with similarly labeled cells were also grown for eight days (two passages) in 40 μM L-lysine (H) and 10 mM DAP (L) and were analyzed as above (bottom panels). Species-nonspecific peptides were ignored. Each timepoint depicts a single sample processed by LC-MS/MS.

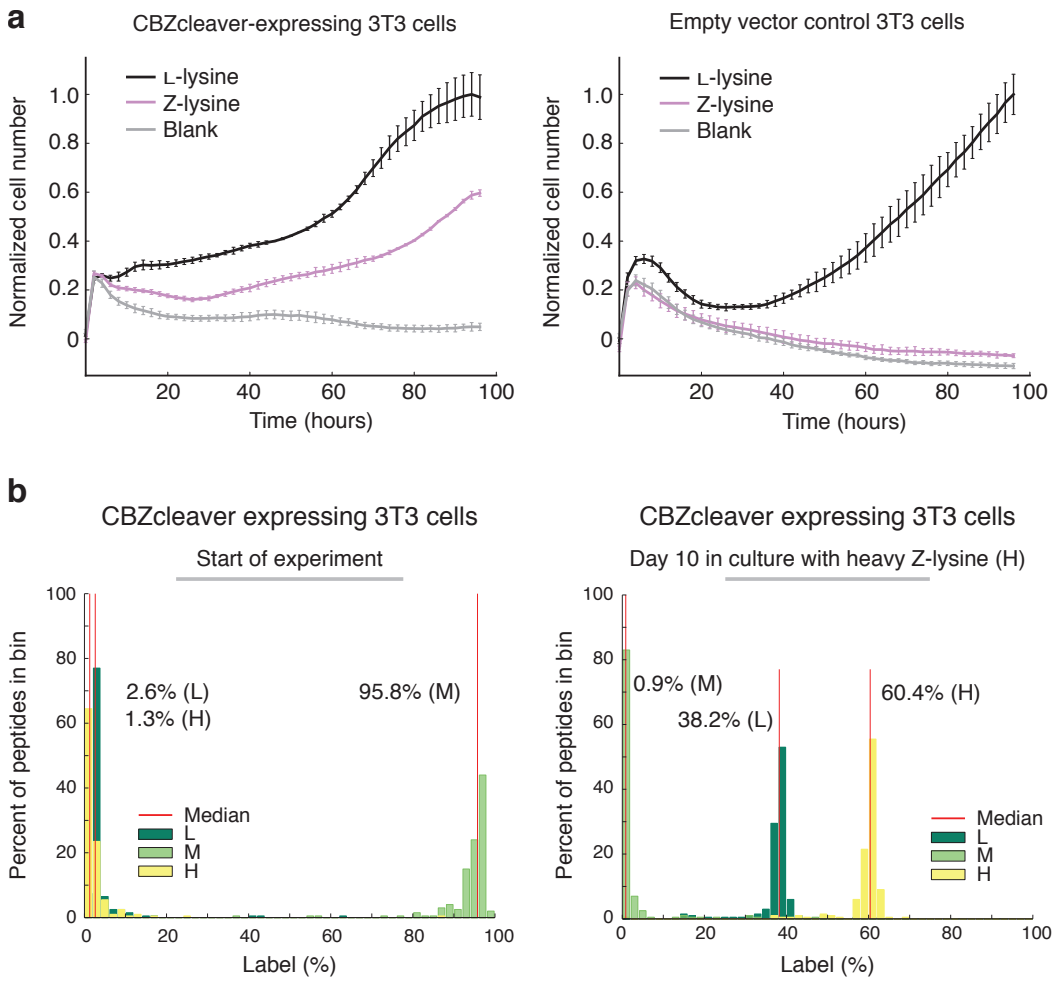

Supplementary Figure 19: **3T3 cells expressing the CBZcleaver enzyme grow suboptimally on Z-lysine and partially incorporate L-lysine produced from Z-lysine (N^{α}-Cbz-L-lysine).** (**a**) 3T3 cells stably transfected with CBZcleaver (left panel) or empty control vector (right panel) were cultured in 0.798 mM L-lysine, 2.5 mM Z-lysine, or without either (blank). Cell growth was estimated by the impedance-based xCELLigence assay and data was normalized to maximum values for each cell-type. Error bars represent the standard deviation of three biological replicates. (**b**) Peptide histograms depicting the light L-lysine (L), medium L-lysine (M), and heavy L-lysine (H) status of the 200 most intense peptides (that contain L-lysine) in CBZcleaver-expressing 3T3 cells. The labeling status was assessed by quantitative LC-MS/MS at the beginning of the experiment where the cells were labeled with medium L-lysine (left, M) and after 10 days (two passages) in L-lysine-free media with heavy labeled Z-lysine (right, H). For synthesis of heavy Z-lysine, see **Supplementary Methods**. The percent label incorporation for the median peptide is indicated (red bars). Concentration of L-lysine (M) used was 0.798 mM, and Z-lysine (H) was 2.5 mM. Although specific to CBZcleaver-expressing cells, both growth on Z-lysine and L-lysine incorporation based on Z-lysine were incomplete, and therefore, we discontinued further experimentation with the CBZcleaver-Z-lysine enzyme-precursor pair. Each plot depicts a single sample processed by LC-MS/MS.

Supplementary Tables

Supplementary Table 1: **Transgenic cell lines and the precursor-enzyme pairs used for mass spectrometry studies.** Da, Dalton; DAP, 2,6-diaminopimelic acid; DDC, Diaminopimelate decarboxylase; lyr, lysine racemase; * heavy form (deuterated).

Cell type (origin)	**Enzyme** (origin)	**Precursor of L-lysine**	**Mass difference**
MDA-MB-231 (human breast adenocarcinoma)	lyr (*P. mirabilis*)	D-lysine D-lysine*	0 Da 8 Da
HEK293T (human embryonic kidney)	DDC (*A. thaliana*)	DAP	0 Da
3T3 (mouse embryonic fibroblast)	DDC (*A. thaliana*)	DAP	0 Da

Supplementary Table 2: **Growth of various cell lines using CTAP enzyme-precursor pairs.** Qualitative estimates of cell growth on 10 mM DAP or 4 mM D-lysine compared to growth on standard levels of L-lysine (0.798 mM in DMEM). As indicated, each human or mouse cell line transgenically expresses CTAP enzymes DDC or lyr. The time to reach normal growth rates varied between cell-types from immediate to a short passaging/selection period, indicating that certain cell-types may be more readily applicable to this method. "+++" indicates similar growth rate to that of L-lysine, "++" slightly lower growth rate, "+" considerably slower growth, and "-" no growth. Note that rescue was confined to the expected enzyme-precursor pairs.

Cell line	**Type**	**Origin**	**enzyme:**	***lyr***	**DDC**	***lyr***	**DDC**
			supplemented precursor:	**D-lysine**	**DAP**	**DAP**	**D-lysine**
3T3	Embryonic Fibroblast	Mouse		+++	+++	-	-
B16	Melanoma	Mouse		+++	+	-	-
HEK293T	Embryonic Kidney	Human		+++	+++	-	-
MDA-MB-231	Breast Adenocarcinoma	Human		+++	+++	-	-
THP1	Monocytic Leukemia	Human		+++	++	-	-

Supplementary Table 3: **Incorporation levels of fully labeled cells based on counting light and heavy peaks.** In this majority of this work, we use the robust MaxQuant-based ratios to determine the light and heavy label enrichment. Alternatively, if a particular sample is completely labeled light or heavy, the sample can be analyzed without the default MaxQuant "requantify" and labeling levels can be estimated by the number of total identified light and heavy peaks (intensity L > 0, intensity H > 0). This approach was used to analyze cells labeled with heavy (H) and light (L) L-lysine, respectively (samples from, **Fig. 2cd**, **top panels**). Note that label enrichment levels are close or slightly higher than using H/L ratios (compare with "All peptides" rows in **Supplementary Table 4** below).

Sample	**Label**	**# of Light peaks**	**# of Heavy peaks**	**Light (%)**	**Heavy (%)**
DDC-expressing 3T3 cells	Heavy	88	1495	5.56	94.44
Lyr-expressing MDA-MB-231 cells	Light	1707	19	98.90	1.10

Supplementary Table 4: **Changing parameters has little effect on estimated level of label incorporation.** To test if processing of the MaxQuant output data (peptides.txt) would influence the reported levels of labeling enrichment, we partitioned the data using different filters and recalculated the median H/L ratio and the associated levels of percent heavy and light label. Top: all events above median value; Bottom: all events below media value; PEP: posterior error probability of peptide identification; score: Andromeda score for best associated MS/MS spectrum [1,2].

Parameter	Partition	$\log_2$(H/L ratio)	N	Light (%)	Heavy (%)
DDC-expressing 3T3 cells, labeled with heavy L-lysine (H) (Fig 2c top panel)					
All peptides	all	4.02	1178	5.81	94.19
Intensity	top	4.60	589	3.96	96.04
Intensity	bottom	3.58	589	7.72	92.28
Length	$\geq$14	3.90	541	6.26	93.74
Length	$\leq$13	4.13	637	5.40	94.60
Charges	$\geq$3	4.04	484	5.71	94.29
Charges	$\leq$2	4.00	694	5.89	94.11
PEP	bottom	4.09	589	5.54	94.46
PEP	top	3.97	589	5.98	94.02
Score	top	4.28	589	4.89	95.11
Score	bottom	3.81	589	6.63	93.37
Lyr-expressing MDA-MB-231 cells, labeled with light L-lysine (L) (Fig. 2d top panel)					
All peptides	all	-5.45	1391	97.76	2.24
Intensity	top	-5.93	695	98.39	1.61
Intensity	bottom	-5.00	696	96.97	3.03
Length	$\geq$13	-5.33	665	97.58	2.42
Length	$\leq$12	-5.58	726	97.95	2.05
Charges	$\geq$3	-5.63	568	98.02	1.98
Charges	$\leq$2	-5.34	823	97.59	2.41
PEP	bottom	-5.54	696	97.89	2.11
PEP	top	-5.34	695	97.60	2.40
Score	top	-5.61	695	98.00	2.00
Score	bottom	-5.28	696	97.49	2.51

Supplementary Table 5: **Gene Set Enrichment Analysis (GSEA) of DDC-expressing 3T3 cells in L-lysine, DAP, or starved conditions.** To investigate whether pathways are perturbed when growing transgenic cells on precursor, KEGG pathway GSEA was performed using gene expression profiles with all gene probes of DDC-expressing 3T3 cells cultured with 0.798 mM L-lysine, 10 mM DAP, or in starved conditions (no L-lysine or precursor). Listed are KEGG pathway ontologies that were considered significantly altered using default GSEA settings (Nominal p-value < 0.01 and FDR < 0.25). Triplicates of L-lysine versus starved or L-lysine versus DAP was used as the phenotype vector in the GSEA. Size: number of genes in the set defined by the KEGG term; Enrichment score: the degree to which this gene set is overrepresented at the top or bottom of the ranked list of genes in the expression dataset; Nominal p-value: uncorrected for size of the gene set and for multiple testing; FDR q-value: q-value for the false discovery rate.

KEGG pathway	# of Genes	Enrichment Score (ES)	Normalized ES	Nominal p-value	FDR q-value
Starved versus L-lysine					
HSA00591 LINOLEIC ACID METABOLISM	21	0.479	1.533	0	0.250
HSA04614 RENIN ANGIOTENSIN SYSTEM	15	0.544	1.532	0	0.153
HSA00120 BILE ACID BIOSYNTHESIS	30	0.567	1.487	0	0.189
HSA00530 AMINOSUGARS METABOLISM	27	0.655	1.474	0	0.176
HSA00592 ALPHA LINOLENIC ACID METABOLISM	15	0.492	1.426	0	0.211
HSA01032 GLYCAN STRUCTURES DEGRADATION	27	0.677	1.420	0	0.197
HSA01430 CELL COMMUNICATION	112	-0.662	-1.738	0	0.056
HSA04670 LEUKOCYTE TRANSENDOTHELIAL MIGRATION	100	-0.546	-1.696	0	0.056
HSA04060 CYTOKINE CYTOKINE RECEPTOR INTERACTION	214	-0.375	-1.649	0	0.056
HSA00960 ALKALOID BIOSYNTHESIS II	16	-0.563	-1.644	0	0.056
HSA00640 PROPANOATE METABOLISM	27	-0.552	-1.536	0	0.100
HSA04662 B CELL RECEPTOR SIGNALING PATHWAY	56	-0.502	-1.523	0	0.093
HSA04660 T CELL RECEPTOR SIGNALING PATHWAY	84	-0.459	-1.521	0	0.087
HSA04630 JAK STAT SIGNALING PATHWAY	134	-0.363	-1.520	0	0.083
HSA04510 FOCAL ADHESION	168	-0.607	-1.505	0	0.095
HSA05020 PARKINSONS DISEASE	15	-0.712	-1.493	0	0.094
HSA00620 PYRUVATE METABOLISM	34	-0.499	-1.465	0	0.106
HSA04360 AXON GUIDANCE	113	-0.464	-1.461	0	0.098
HSA02010 ABC TRANSPORTERS GENERAL	37	-0.419	-1.453	0	0.107
HSA04512 ECM RECEPTOR INTERACTION	74	-0.683	-1.436	0	0.128
HSA04020 CALCIUM SIGNALING PATHWAY	150	-0.344	-1.428	0	0.130
HSA05217 BASAL CELL CARCINOMA	50	-0.344	-1.410	0	0.149
HSA05210 COLORECTAL CANCER	76	-0.497	-1.404	0	0.152
HSA04540 GAP JUNCTION	75	-0.486	-1.399	0	0.151
HSA00410 BETA ALANINE METABOLISM	24	-0.465	-1.395	0	0.156
HSA04640 HEMATOPOIETIC CELL LINEAGE	63	-0.352	-1.389	0	0.160
HSA04520 ADHERENS JUNCTION	65	-0.465	-1.370	0	0.175
HSA00650 BUTANOATE METABOLISM	41	-0.464	-1.352	0	0.183
HSA00360 PHENYLALANINE METABOLISM	25	-0.413	-1.335	0	0.194
HSA00071 FATTY ACID METABOLISM	39	-0.485	-1.332	0	0.186
HSA00280 VALINE LEUCINE AND ISOLEUCINE DEGRADATION	39	-0.464	-1.316	0	0.198
HSA00532 CHONDROITIN SULFATE BIOSYNTHESIS	16	-0.439	-1.313	0	0.196
DAP versus L-lysine					
No significant changes					

Supplementary Table 6: **Gene Set Enrichment Analysis (GSEA) of lyr-expressing MDA-MB-231 cells in L-lysine, D-lysine, or starved conditions.** To investigate the global effect of growing cells on precursors, KEGG pathway GSEA was performed using gene expression profiles of all gene probes of lyr-expressing MDA-MB-231 cells cultured with 0.798 mM L-lysine, 4 mM D-lysine, or in starved condition, in a similar manner as stated in **Supplementary Table 5**.

KEGG pathway	# of Genes	Enrichment Score (ES)	Normalized ES	Nominal p-value	FDR q-value
Starved versus L-lysine					
HSA04610 COMPLEMENT AND COAGULATION CASCADES	69	0.528	1.818	0	0.055
HSA04060 CYTOKINE CYTOKINE RECEPTOR INTERACTION	255	0.517	1.738	0	0.055
HSA04612 ANTIGEN PROCESSING AND PRESENTATION	83	0.595	1.606	0	0.071
HSA04650 NATURAL KILLER CELL MEDIATED CYTOTOXICITY	132	0.526	1.592	0	0.067
HSA00260 GLYCINE SERINE AND THREONINE METABOLISM	45	0.615	1.588	0	0.065
HSA04640 HEMATOPOIETIC CELL LINEAGE	87	0.434	1.584	0	0.063
HSA04514 CELL ADHESION MOLECULES	134	0.566	1.551	0	0.062
HSA02010 ABC TRANSPORTERS GENERAL	44	0.499	1.535	0	0.061
HSA04940 TYPE I DIABETES MELLITUS	45	0.768	1.508	0	0.076
HSA04920 ADIPOCYTOKINE SIGNALING PATHWAY	72	0.600	1.495	0	0.074
HSA04140 REGULATION OF AUTOPHAGY	29	0.637	1.489	0	0.072
HSA00530 AMINOSUGARS METABOLISM	29	0.733	1.476	0	0.077
HSA04080 NEUROACTIVE LIGAND RECEPTOR INTERACTION	244	0.269	1.464	0	0.086
HSA05120 EPITHELIAL CELL SIGNALING IN H PYLORI INFECTION	67	0.667	1.441	0	0.098
HSA04020 CALCIUM SIGNALING PATHWAY	173	0.415	1.428	0	0.117
HSA00760 NICOTINATE AND NICOTINAMIDE METABOLISM	23	0.574	1.407	0	0.142
HSA00272 CYSTEINE METABOLISM	17	0.662	1.395	0	0.149
HSA00565 ETHER LIPID METABOLISM	30	0.533	1.378	0	0.174
HSA04010 MAPK SIGNALING PATHWAY	256	0.446	1.370	0	0.185
HSA04630 JAK STAT SIGNALING PATHWAY	153	0.434	1.369	0	0.179
HSA00531 GLYCOSAMINOGLYCAN DEGRADATION	17	0.736	1.361	0	0.182
HSA04910 INSULIN SIGNALING PATHWAY	134	0.503	1.357	0	0.177
HSA04150 MTOR SIGNALING PATHWAY	45	0.505	1.353	0	0.177
HSA04930 TYPE II DIABETES MELLITUS	44	0.462	1.349	0	0.222
HSA04370 VEGF SIGNALING PATHWAY	70	0.495	1.335	0	0.230
HSA00980 METABOLISM OF XENOBIOTICS BY CYTOCHROME P450	70	0.368	1.333	0	0.225
HSA04742 TASTE TRANSDUCTION	51	0.259	1.333	0	0.219
HSA04210 APOPTOSIS	82	0.539	1.332	0	0.215
HSA04130 SNARE INTERACTIONS IN VESICULAR TRANSPORT	35	0.675	1.331	0	0.213
HSA01032 GLYCAN STRUCTURES DEGRADATION	30	0.773	1.315	0	0.218
HSA01430 CELL COMMUNICATION	138	0.340	1.304	0	0.226
HSA04070 PHOSPHATIDYLINOSITOL SIGNALING SYSTEM	77	0.493	1.298	0	0.233
HSA00532 CHONDROITIN SULFATE BIOSYNTHESIS	17	0.622	1.294	0	0.237
HSA00511 N GLYCAN DEGRADATION	16	0.822	1.289	0	0.234
HSA00562 INOSITOL PHOSPHATE METABOLISM	50	0.471	1.288	0	0.237
D-lysine versus L-lysine					
No significant changes					

Supplementary Table 7: **Primers and reactions for cloning of lyr.** Note that the clamp / extra sequences are italicized and the restriction enzyme sites are highlighted in lowercase bold. Gene sequences are all uppercase and the P2A sequence is in lowercase.

Reaction	Primer Name	Oligonucleotide Sequence (5'→3')	Product Size
Subclone lyr into pLM-mCherry from GeneArt synthesized lyr construct			
1	FWD-FluorescentGene-AgeI	*CCGGTT***accggt**ATGGTGAGCAAGGGCGAGGAG	786nt
	REV-P2A-FluorescentGene	agggccgggattctcctccacgtcacctgcttgtt tgagtagtgagaagtttgttgctccagatccCTTG TACAGCTCGTCCATGCCG	
2	FWD-P2A-lyr	ggatctggagcaacaaacttctcactactcaaaca agcaggtgacgtggaggagaatcccggccctATGA GCCTGGGCATCAGATAC	1300nt
	REV-lyr-SalI	*TGTT***gtcgac**TCAATCCACCAGCACGCG	
3	FWD-FluorescentGene-AgeI	*CCGGTT***accggt**ATGGTGAGCAAGGGCGAGGAG	2020nt
	REV-lyr-SalI	*TGTT***gtcgac**TCAATCCACCAGCACGCG	

Three PCR reactions were to generate pLM-mCherry-P2A-lyr for insert into pLM using the AgeI and SalI restriction enzymes. In the first reaction, a mCherry-P2A oligonucleotide fusion that began with an AgeI site was created. The second reaction generated a PCR fragment of P2A-lyr flanked by SalI. Finally, an overlapping PCR reaction created AgeI-mCherry-P2A-lyr-SalI. This sequence was then ligated into the AgeI-SalI digested pLM vector.

Subclone truncated lyr into pLM-mCherry from GeneArt synthesized lyr construct			
1	FWD-FluorescentGene-AgeI	*CCGGTT***accggt**ATGGTGAGCAAGGGCGAGGAG	786nt
	REV-P2A-FluorescentGene	agggccgggattctcctccacgtcacctgcttgtt tgagtagtgagaagtttgttgctccagatccCTTG TACAGCTCGTCCATGCCG	
2	FWD-P2A-truncate.lyr	ggatctggagcaacaaacttctcactactcaaaca agcaggtgacgtggaggagaatcccggccctATGC AGCAGCCCGTGAACTACAACC	1264nt
	REV-lyr.HIS-SalI	*AGTT***gtcgac**TCAGTGGTGATGGTGATGATGATCC ACCAGCACGCGCTG	
3	FWD-FluorescentGene-AgeI	*CCGGTT***accggt**ATGGTGAGCAAGGGCGAGGAG	1984nt
	REV-lyr.HIS-SalI	*AGTT***gtcgac**TCAGTGGTGATGGTGATGATGATCC ACCAGCACGCGCTG	

Three PCR reactions were to generate pLM-mCherry-P2A-lyr for insert into pLM using the AgeI and SalI restriction enzymes. In the first reaction, a mCherry-P2A oligonucleotide fusion that began with an AgeI site was created. The second reaction generated a PCR fragment of P2A-lyr flanked by SalI. This lyr construct contains a HIS-tag on the C-terminal and was truncated 18 amino acids on the N-terminal. Finally, an overlapping PCR reaction created AgeI-mCherry-P2A-lyr-SalI. This sequence was then ligated into the AgeI-SalI digested pLM vector.

Fuse mCherry to truncated lyr in pLM			
1	FWD-LINK-lyr	agcggtagcATGCAGCAGCCCGTGAACTA	8575nt
	REV-LINK-FluorescentGene	gccgctaccCTTGTACAGCTCGTCCATGC	

Using the pLM vector with truncated lyr (see above), a single PCR reaction was performed with high fidelity Accuprime Pfx polymerase (Invitrogen) to delete the P2A site, insert a short 6 amino acid linker between mCherry and truncated lyr, and amplify the entire vector. Both primers contain 5' phosphates and the linker sequence is underlined.

Prepend mitochondrial targeting sequence (MTS) to mCherry-lyr fusion in pLM			
1	FWD-AgeI-MTS	*CGT***accggt**ATGTCCGTCCTGACGCCGCTGCT	125nt
	REV-AgeI-MTS	*GT***accggt**GGTGGCGACAGGAGGATCCCCcaacga atggat	

The mitochondrial targeting sequence (MTS) was amplified with AgeI sites on both 3' and 5' ends. This sequence was then digested with AgeI and ligated into the AgeI-digested pLM vector that contained mCherry fused to truncated lyr (see above). The linker sequence between MTS and mCherry is underlined.

Supplementary Table 8: **Primers and reactions for cloning of DDC.** Note that the clamp / extra sequences are italicized and the restriction enzyme sites are highlighted in lowercase bold. Gene sequences are all uppercase and the P2A sequence is in lowercase.

Reaction	Primer Name	Oligonucleotide Sequence (5'→3')	Product Size
Clone DDC (TAIR id = AT3G14390) from *Arabidopsis thaliana* cDNA			
1	FWD-DDC-XhoI	*GCC***ctcgag**ATGGCGGCAGCTACTCAAT	1475nt
	REV-DDC-EcoRI	*CGC***gaattc**GTTCATAGACCTTCAAAGAAACGC	
Subclone DDC into MSCV-IRES-GFP (pMIG)			
1	FWD-DDC-EcoRI	*ATC***gaattc**ATGGCGGCAGCTACTCAAT	1475nt
	REV-DDC-EcoRI	*CGC***gaattc**GTTCATAGACCTTCAAAGAAACGC	
Subclone DDC into pLM-GFP			
1	FWD-FluorescentGene-AgeI	*CCGGTT***accggt**ATGGTGAGCAAGGGCGAGGAG	795nt
	REV-P2A-FluorescentGene	agggccgggattctcctccacgtcacctgcttgtt tgagtagtgagaagtttgttgctccagatccCTTG TACAGCTCGTCCATGCCG	
2	FWD-P2A-DDC	ggatctggagcaacaaacttctcactactcaaaca agcaggtgacgtggaggagaatcccggccctATGG CGGCAGCTACTCAAT	1533nt
	REV-DDC-SalI	*CCGGTT***gtcgac**TCATAGACCTTCAAAGAAACGCA	
3	FWD-FluorescentGene-AgeI	*CCGGTT***accggt**ATGGTGAGCAAGGGCGAGGAG	2262nt
	REV-DDC-SalI	*CCGGTT***gtcgac**TCATAGACCTTCAAAGAAACGCA	

Three PCR reactions were to generate pLM-GFP-P2A-DDC for insert into pLM using the AgeI and SalI restriction enzymes. In the first reaction, a GFP-P2A oligonucleotide fusion that began with an AgeI site was created. The second reaction generated a PCR fragment of P2A-DDC flanked by SalI. Finally, an overlapping PCR reaction created AgeI-GFP-P2A-DDC-SalI. This sequence was then ligated into the AgeI-SalI digested pLM vector.

Supplementary Note 1: Enzyme Sequences

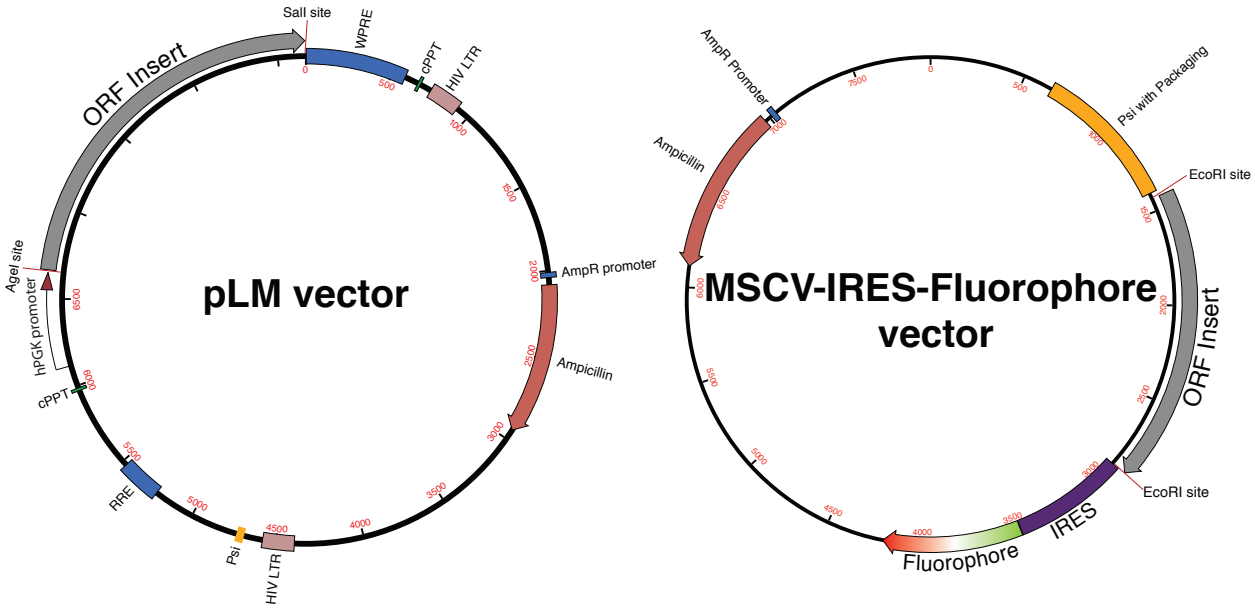

Overview of the two vector backbones used in this study. DDC, lyr, CBZcleaver, and wild-type lyr were inserted into pLM and/or MSCV-IRES-Fluoraphore vector backbones. The lentiviral backbone pLM was used for infections of human MDA-MB-231 and HEK293T cell lines. For infection of mouse 3T3 cells, we utilized the MSCV retroviral backbone containing either IRES-GFP or IRES-mCherry. Above are general schematics of each vector and the following pages contain detailed schematics and sequences for each of the inserts.

Constructs generated:

1. **lyr** (pLM-MTS-mCherry-lyr$^{\triangle 4\text{-}57nt}$)
2. **DDC** (pLM-GFP-P2A-DDC)
3. **DDC** (MSCV-DDC-IRES-GFP)
4. **CBZcleaver** (MSCV-CBZcleaver-IRES-mCherry)
5. **Wild-type lyr** (pLM-mCherry-P2A-Wild-type lyr)

Supplementary Sequence 1: **Lysine racemase (lyr), truncated and fused to mCherry containing a mitochondrial targeting sequence**

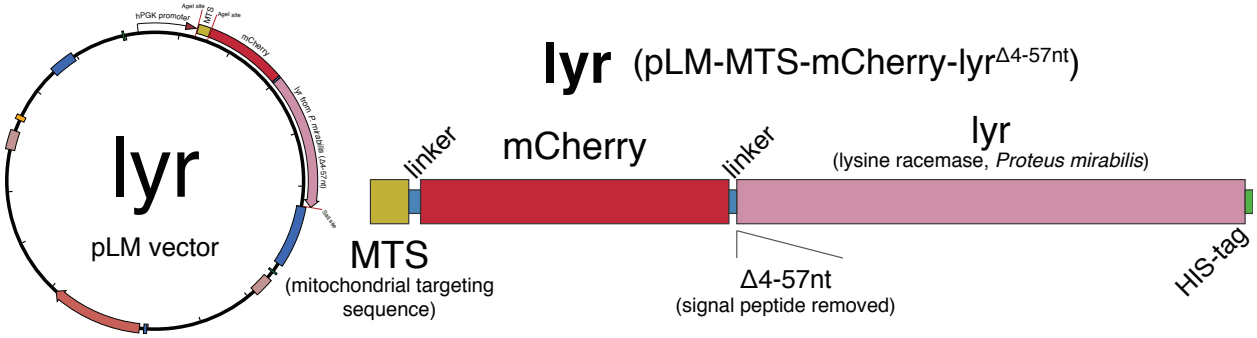

Note: The colors of the sequence are as depicted in the schematic. The mitochondrial targeting sequence (MTS), mCherry, truncated-lyr, and HIS-tagged sequences are in lowercase and the linker regions are shown in uppercase.

>lyr (modified) from *Proteus mirabilis* as cloned in the pLM vector

atgtccgtcctgacgccgctgctgctgcggggcttgacaggctcggcccggcggctcccagtgccgcgcgccaagatcca
ttcgttgGGGGATCCTCCTGTCGCCACCACCGGTatggtgagcaagggcgaggaggataacatggccatcatcaaggagt
tcatgcgcttcaaggtgcacatggagggctccgtgaacggccacgagttcgagatcgagggcgagggcgagggccgcccc
tacgagggcacccagaccgccaagctgaaggtgaccaagggtggcccccctgcccttcgcctgggacatcctgtcccctca
gttcatgtacggctccaaggcctacgtgaagcaccccgccgacatccccgactacttgaagctgtccttccccgagggct
tcaagtgggagcgcgtgatgaacttcgaggacggcggcgtggtgaccgtgacccaggactcctccctgcaggacggcgag
ttcatctacaaggtgaagctgcgcggcaccaacttcccctccgacggccccgtaatgcagaagaagaccatgggctggga
ggcctcctccgagcggatgtaccccgaggacggcgccctgaagggcgagatcaagcagaggctgaagctgaaggacggcg
gccactacgacgctgaggtcaagaccacctacaaggccaagaagcccgtgcagctgcccggcgcctacaacgtcaacatc
aagttggacatcacctcccacaacgaggactacaccatcgtggaacagtacgaacgcgccgagggccgccactccaccgg
cggcatggacgagctgtacaagGGTAGCGGCAGCGGTAGCatgcagcagcccgtgaactacaacccccctgccacacagg
tggcccaggtgcagcctgccatcgtgaacaacagctggatcgagatcagcagaagcgccctggacttcaacgtgaagaag
gtgcagagcctgctgggcaagcagagcagcctgtgtgctgtgctgaagggcgacgcctacggccacgatctgtctctggt
ggcccccatcatgatcgagaacaatgtgaagtgcatcggcgtgaccaacaaccaggaactgaaagaagtgcgggacctgg
gcttcaagggcagactgatgagagtgcggaacgccaccgagcaggaaatggcccaggccaccaactacaacgtggaagaa
ctgatcggcgacctggacatggccaagagactggacgctatcgccaagcagcagaacaaagtgatccccatccacctggc
tctgaacagcggcggcatgagcagaaacggcctggaagtggacaacaagtctggcctggaaaaggccaagcagatctccc
agctggccaacctgaaggtcgtgggcatcatgagccactaccccgaagaggacgccaacaaagtgcgcgaggacctggcc
cggtttaagcagcagtctcagcaggtgctggaagtgatgggcctggaacggaacaacgtgaccctgcacatggctaacac
cttcgccaccatcaccgtgcccgagagctggctggatatggtgcgagtgggcggcatcttctacggcgacacaatcgcca
gcaccgactacaagagagtgatgaccttcaagagcaatatcgcctccatcaactactaccccaagggcaacaccgtgggc
tacgacagaacctacaccctgaagagggacagcgtgctggctaacatccccgtgggatacgccgacggctacagaagagt
gttcagcaacgccggccacgccctgatcgctggacagagggtgccagtgctgggaaagaccagcatgaacaccgtgatcg
tggacatcaccagcctgaacaacatcaagcccggcgacgaggtggtgttcttcggcaagcagggcaacagcgagatcacc
gccgaggaaatcgaggacatctctggcgccctgttcaccgagatgagcatcctgtggggcgccaccaatcagcgcgtgct
ggtggatcatcatcaccatcaccactga

Supplementary Sequence 2: **Diaminopimelate decarboxylase (DDC) from *Arabidopsis thaliana* in the pLM vector**

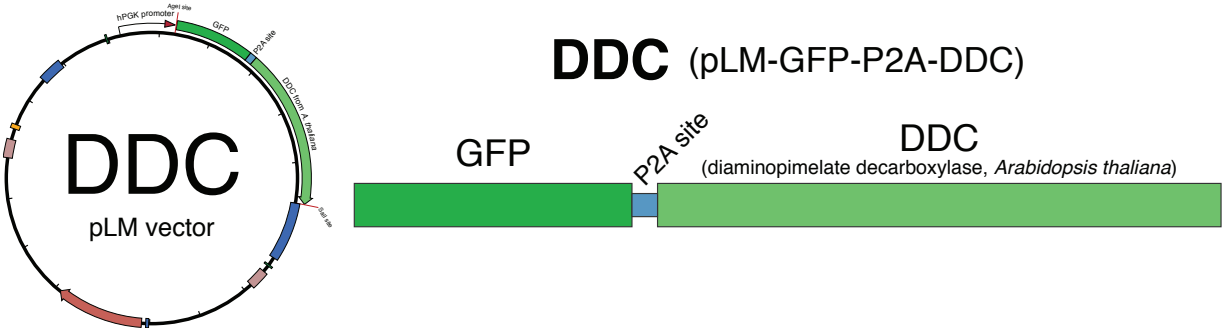

Note: The DDC gene was cloned directly from *A. thaliana* cDNA using the primers in **Table 8**. Please see AT3G14390 at the Arabidopsis Information Resource (TAIR) for more information about *A. thaliana* DDC. The colors of the sequence are as depicted in the schematic. GFP and DDC sequences are in lowercase and the P2A site is in uppercase.

>DDC from *Arabidopsis thaliana* as cloned in the pLM vector

atggtgagcaagggcgaggagctgttcaccggggtggtgcccatcctggtcgagctggacggcgacgtaaacggccacaa
gttcagcgtgtctggcgagggcgagggcgatgccacctacggcaagctgaccctgaagttcatctgcaccaccggcaagc
tgcccgtgccctggcccaccctcgtgaccaccctgacctacggcgtgcagtgcttcagccgctaccccgaccacatgaag
cagcacgacttcttcaagtccgccatgcccgaaggctacgtccaggagcgcaccatcttcttcaaggacgacggcaacta
caagacccgcgccgaggtgaagttcgagggcgacaccctggtgaaccgcatcgagctgaagggcatcgacttcaaggagg
acggcaacatcctggggcacaagctggagtacaactacaacagccacaacgtctatatcatggccgacaagcagaagaac
ggcatcaaggcgaacttcaagatccgccacaacatcgaggacggcagcgtgcagctcgccgaccactaccagcagaacac
ccccatcggcgacggccccgtgctgctgcccgacaaccactacctgagcacccagtccgccctgagcaaagaccccaacg
agaagcgcgatcacatggtcctgctggagttcgtgaccgccgccgggatcactctcggcatggacgagctgtacaagGGA
TCTGGAGCAACAAACTTCTCACTACTCAAACAAGCAGGTGACGTGGAGGAGAATCCCGGCCCTatggcggcagctactca
atttctctcccaaccttcgtctctcaatccacaccaactgaagaaccaaacctcacaacgctccagaagcatccctgtct
tgtctcttaaatccacattgaagccacttaaacgcctctccgtgaaagccgccgtcgtttctcaaaactcgtccaaaacc
gtgacgaagttcgatcactgtttcaagaaatcatcagatgggtttctctattgtgaaggaactaaagttgaggatatcat
ggagtcagtggagagaagacccttttacttatatagcaaacctcagatcactagaaacctcgaggcttataaagaagcat
tggaaggagtgagctctgtgattggttacgctatcaaagctaataacaatcttaaaattttggagcatttgagaagttta
ggctgtggtgctgtgctcgttagtggaaatgagcttagacttgctcttcgtgctggtttcgatcccacaaagtgcatttt
caatggaaatggcaagtctttggaagatttagttctagctgctcaagaaggtgttttcgttaatgtcgatagtgagtttg
acttgaataacattgtggaagcttcaagaatttctggtaagcaggtcaatgtactgctgcgtatcaatcctgatgttgat
cctcaggtgcatccatatgttgctactgggaacaagaactcaaagtttggtatcaggaacgagaagcttcaatggtttct
ggatcaggtcaaggcacatcccaaagagctgaagcttgttggagctcattgccatctaggctctaccattactaaggtgg
atatattcagagatgcggcagttctcatgatagaatacattgacgagatccggcgtcaaggttttgaagttagttacttg
aacattggtggtggtttagggattgattattaccatgccggcgctgtccttcccacacccatggatctcatcaacactgt
aagagagcttgttctttcacgagacctgaatctaataatcgagccagggagatctctgattgcaaacacttgctgtttcg
tcaaccatgtaactggtgtgaagacgaatggaactaagaacttcatagtcattgatggaagtatggctgagcttatccgt
cccagtctttatgatgcttatcagcacattgagttggtctctcctccaccggctgaagcagaggttaccaaattcgacgt
agtgggtcctgtctgtgaatctgctgatttcctgggcaaagacagagagcttcccactcctccacagggagctggtctgg
tggttcatgacgctggtgcatactgtatgagcatggcttccacttacaatctcaagatgcgtcctccggaatactgggtt
gaagaagatgggtcgatcactaagataaggcatgctgagacattcgatgaccatttgcgtttctttgaaggtctatga

Supplementary Sequence 3: **Diaminopimelate decarboxylase (DDC) from *Arabidopsis thaliana* in the MSCV-IRES-GFP vector**

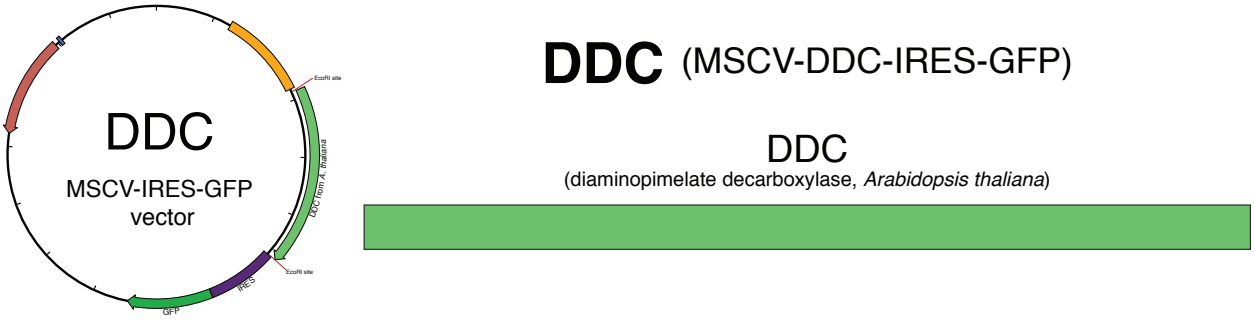

Note: This the same DDC sequence as is contained in the pLM vector above. The MSCV vector carries DDC directly upstream of IRES-GFP (whereas the pLM vector contains DDC in frame downstream of GFP-P2A).

>DDC from *Arabidopsis thaliana* as cloned in the MSCV-IRES-GFP vector

atggcggcagctactcaatttctctcccaaccttcgtctctcaatccacaccaactgaagaaccaaacctcacaacgctc
cagaagcatccctgtcttgtctcttaaatccacattgaagccacttaaacgcctctccgtgaaagccgccgtcgtttctc
aaaactcgtccaaaaccgtgacgaagttcgatcactgtttcaagaaatcatcagatgggtttctctattgtgaaggaact
aaagttgaggatatcatggagtcagtggagagaagacccttttacttatatagcaaacctcagatcactagaaacctcga
ggcttataaagaagcattggaaggagtgagctctgtgattggttacgctatcaaagctaataacaatcttaaaattttgg
agcatttgagaagtttaggctgtggtgctgtgctcgttagtggaaatgagcttagacttgctcttcgtgctggtttcgat
cccacaaagtgcattttcaatggaaatggcaagtctttggaagatttagttctagctgctcaagaaggtgttttcgttaa
tgtcgatagtgagtttgacttgaataacattgtggaagcttcaagaatttctggtaagcaggtcaatgtactgctgcgta
tcaatcctgatgttgatcctcaggtgcatccatatgttgctactgggaacaagaactcaaagtttggtatcaggaacgag
aagcttcaatggtttctggatcaggtcaaggcacatcccaaagagctgaagcttgttggagctcattgccatctaggctc
taccattactaaggtggatatattcagagatgcggcagttctcatgatagaatacattgacgagatccggcgtcaaggtt
ttgaagttagttacttgaacattggtggtggtttagggattgattattaccatgccggcgctgtccttcccacacccatg
gatctcatcaacactgtaagagagcttgttctttcacgagacctgaatctaataatcgagccagggagatctctgattgc
aaacacttgctgtttcgtcaaccatgtaactggtgtgaagacgaatggaactaagaacttcatagtcattgatggaagta
tggctgagcttatccgtcccagtctttatgatgcttatcagcacattgagttggtctctcctccaccggctgaagcagag
gttaccaaattcgacgtagtgggtcctgtctgtgaatctgctgatttcctgggcaaagacagagagcttcccactcctcc
acagggagctggtctggtggttcatgacgctggtgcatactgtatgagcatggcttccacttacaatctcaagatgcgtc
ctccggaatactgggttgaagaagatgggtcgatcactaagataaggcatgctgagacattcgatgaccatttgcgtttc
tttgaaggtctatga

Supplementary Sequence 4: **CBZcleaver from *Sphingomonas paucimobilis* in the MSCV-IRES-mCherry vecotr as synthesized by GeneArt (sequence optimized for mouse expression)**

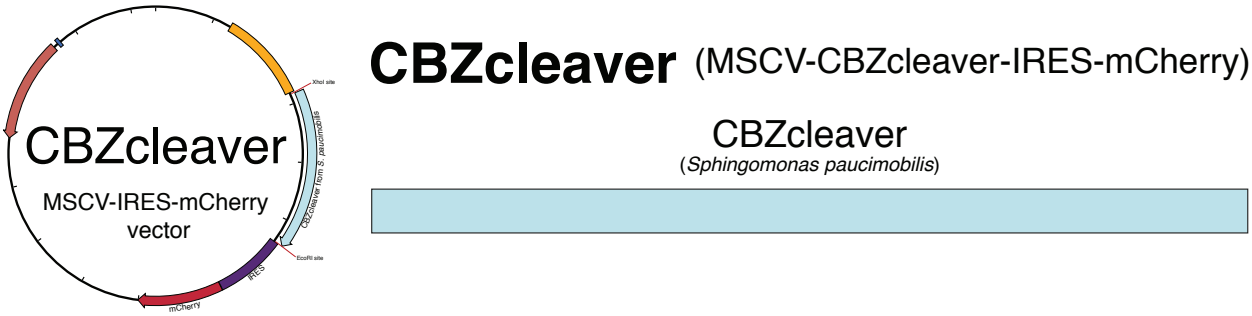

Note: The CBZcleaver enzyme lies directly upstream of IRES-mCherry in this MSCV vector.

>CBZcleaver from *Sphingomonas paucimobilis* as cloned in the MSCV-IRES-mCherry vector

```
atggtgcagcccacccctacccctcagagcgagctgcctggcctgatcgccagagacatggaaggcctgatgacactgta
cagggacctgcacgccaaccccgagctgagcctgcaggaagtgaacaccgccgccaagctggccaagagactgaaggcca
tgaagttcgacgtgacagagaaagtgggcggcaccggcgtggtggccgtgatgaagaacggcagcggacctgtgctgctg
atcagagccgatatggacggcctgcccgtggtggaacagaccggcctggacttcgccagcaaagtgcggaccaagacccc
cgagggcgtggaaacaggcgtgatgcacgcttgcggccacgacacccacatgaccgccttcatcgagacagccaagctgc
tgagcagccagaaagacaagtggaagggcaccctggtgatgatcctgcagcccgccgaggaagtgggcaagggcgccagg
gacatgctggaagatggcctgtacaccagattccccagacccacccacgctatcgccttccacgacgccgccaacctcca
ggctggcgtggtgggatacacccctggctacgccctggccaacgtggacagcgtggacatcgtggtgaaaggcctgggag
gacacggcgcctacccccagaccaccagagatcccatcgtgctgggcagcagaatcgtgaccagcctgcagaccctggtg
tccagagagcaggacccccaggaccctgccgtggtgacagtgggctctttccaggctggcgccaagcacaacatcatccc
cgaccaggctctgctgctgctgaccgtgcggagctacagcgacgagacaagagccaagctgatcaagggcatcgagagaa
tcgccagaggcgaggctatcgccgctggcgtgcccgacgacaagatgcctgtggtgtccgtgaaggacgagttcaccccc
agcacctacaacccccccgagttcgccgagcagatgggcgctctgctgaagggacacttcgccgagggcagagtggtgaa
aacccctgccgtgatgggcggcgaggacttcggcagattctacagagccgacaagtctatcaacagcttcatcttctggg
tgggaggcgtgccagccgataagatggccgctgcccaggccggccagatcacactgcctagcctgcacagccctttctgg
gcccctgaggccgacaaagtgatcgccaccgccagcgaggccatgaccgtgctggccatggacatcctgaagaaggactg
a
```

Supplementary Sequence 5: **Full length lysine racemase (wild-type lyr) from *Proteus mirabilis* as synthesized by GeneArt (nucleotide sequence optimized for Mouse expression by GeneArt)**

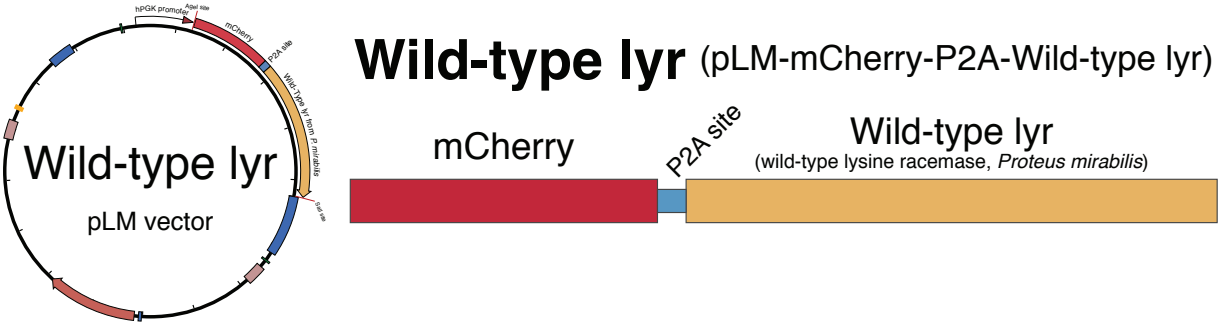

Note: The colors of the sequence are as depicted in the schematic above. mCherry and non-truncated lyr sequences are in lowercase and the P2A site is in uppercase.

>wild-type lyr from *Proteus mirabilis* as cloned in the pLM vector

atggtgagcaagggcgaggaggataacatggccatcatcaaggagttcatgcgcttcaaggtgcacatggagggctccgt
gaacggccacgagttcgagatcgagggcgagggcgagggccgcccctacgagggcacccagaccgccaagctgaaggtga
ccaagggtggcccccctgcccttcgcctgggacatcctgtcccctcagttcatgtacggctccaaggcctacgtgaagcac
cccgccgacatccccgactacttgaagctgtccttccccgagggcttcaagtgggagcgcgtgatgaacttcgaggacgg
cggcgtggtgaccgtgacccaggactcctccctgcaggacggcgagttcatctacaaggtgaagctgcgcggcaccaact
tcccctccgacggccccgtaatgcagaagaagaccatgggctgggaggcctcctccgagcggatgtaccccgaggacggc
gccctgaagggcgagatcaagcagaggctgaagctgaaggacggcggccactacgacgctgaggtcaagaccacctacaa
ggccaagaagcccgtgcagctgcccggcgcctacaacgtcaacatcaagttggacatcacctcccacaacgaggactaca
ccatcgtggaacagtacgaacgcgccgagggccgccactccaccggcggcatggacgagctgtacaagGGATCTGGAGCA
ACAAACTTCTCACTACTCAAACAAGCAGGTGACGTGGAGGAGAATCCCGGCCCTatgagcctgggcatcagatacctggc
cctgctgcccctgttcgtgatcaccgcttgtcagcagcccgtgaactacaaccccctgccacacaggtggcccaggtgc
agcctgccatcgtgaacaacagctggatcgagatcagcagaagcgccctggacttcaacgtgaagaaggtgcagagcctg
ctgggcaagcagagcagcctgtgtgctgtgctgaagggcgacgcctacggccacgatctgtctctggtggcccccatcat
gatcgagaacaatgtgaagtgcatcggcgtgaccaacaaccaggaactgaaagaagtgcgggacctgggcttcaagggca
gactgatgagagtgcggaacgccaccgagcaggaaatggcccaggccaccaactacaacgtggaagaactgatcggcgac
ctggacatggccaagagactggacgctatcgccaagcagcagaacaaagtgatccccatccacctggctctgaacagcgg
cggcatgagcagaaacggcctggaagtggacaacaagtctggcctggaaaaggccaagcagatctcccagctggccaacc
tgaaggtcgtgggcatcatgagccactaccccgaagaggacgccaacaaagtgcgcgaggacctggcccggtttaagcag
cagtctcagcaggtgctggaagtgatgggcctggaacggaacaacgtgaccctgcacatggctaacaccttcgccaccat
caccgtgcccgagagctggctggatatggtgcgagtgggcggcatcttctacggcgacacaatcgccagcaccgactaca
agagagtgatgaccttcaagagcaatatcgcctccatcaactactaccccaagggcaacaccgtgggctacgacagaacc
tacaccctgaagagggacagcgtgctggctaacatccccgtgggatacgccgacggctacagaagagtgttcagcaacgc
cggccacgccctgatcgctggacagagggtgccagtgctgggaaagaccagcatgaacaccgtgatcgtggacatcacca
gcctgaacaacatcaagcccggcgacgaggtggtgttcttcggcaagcagggcaacagcgagatcaccgccgaggaaatc
gaggacatctctggcgccctgttcaccgagatgagcatcctgtggggcgccaccaatcagcgcgtgctggtggattga

Supplementary Note 2: Synthesis of Z-lysine [N^{α}-Cbz-L-lysine(K8)]

To a solution of saturated aqueous $NaHCO_3$ (1.25 mL) and L-lysine·2HCl (250 mg, 1.11 mmol, 1.00 equiv) was added solid $NaHCO_3$ (105 mg, 1.13 equiv, 1.25 mmol) followed by aqueous $CuSO_4$ (1.5 mL, 0.50 M, 0.68 mmol 0.60 equiv), immediately forming a blue copper complex. After stirring for 10 min, di-*tert*-butyl dicarbonate (325 mg, 1.49 mmol, 1.35 equiv) was added in 1 mL acetone. After stirring for 16 h, additional di-*tert*-butyl dicarbonate solid (150 mg, 0.621 equiv, 0.690 mmol) was added. After 24 h, the reaction was quenched with methanol (1 mL) and stirred for an additional 16 h. Ethyl acetate (1 mL) and water (1 mL) were added and the heterogeneous suspension was filtered. The recovered blue solid was taken up in H_2O (3 mL), sonicated for 30 s, and filtered. After air drying, the N^{ϵ}-Boc-protected copper complex was collected as a fine periwinkle blue powder (235 mg, 0.423 mmol, 74.2% yield), which was used without further purification.

To a suspension of N^{ϵ}-Boc-protected copper complex (235 mg, 0.417 mmol, 1.00 equiv) in acetone (1.5 mL) was added 8-hydroxyquinoline (130 mg, 0.900 mmol, 2.13 equiv) and 10% Na_2CO_3 (1.8 mL). After 1 h, *N*-(Benzyloxycarbonyloxy)succinimide (205 mg, 0.821 mmol, 1.97 equiv) in 1 mL acetone was added dropwise over 10 min and stirred for 1 h. The reaction mixture was filtered, and the residue washed with water (3 x 1 mL). The pale green filtrate was acidified carefully with 1 N HCl to a pH of 2, and extracted with ethyl acetate (2 x 5 mL). The combined organics were washed with brine, dried over sodium sulfate, filtered, and concentrated by rotary evaporation to afford crude N^{ϵ}-Boc-N^{α}-Cbz-L-lysine(K8) (148 mg, 45.7% yield, 0.381 mmol), where K8 refers to [$^{13}C_6$,$^{15}N_2$]L-lysine.

To a solution of crude N^{ϵ}-Boc-N^{α}-Cbz-L-lysine(K8) (148 mg, 0.381 mmol, 1.00 equiv) in acetone (1.7 mL) was added TsOH · H_2O (145 mg, 0.762 mmol, 2.00 equiv). After 16 h, crystals were collected by vacuum filtration and washed sparingly with cold acetone, giving N^{α}-Cbz-L-lysine(K8)·TsOH (124 mg, 71.0% yield, 0.270 mmol).

Crude N^{α}-Cbz-L-lysine(K8)·TsOH was dissolved in 1.0 mL 5% acetonitrile (v/v in water), treated with triethylamine (37.5 μL, 0.269 μmol, 1.00 equiv), and purified on a 5.5 g C-18 ISCO RediSep Gold column (5→90% acetonitrile in H_2O). Lyophilization furnished N^{α}-Cbz-L-lysine(K8) as a fluffy white amorphous solid (77 mg, 0.27 mmol, 99% yield).

^{1}H NMR (D_2O, 600 MHz) δ 7.25–7.35 (m, 5H), 5.04 (d, *J* = 12.5 Hz, 1H), 4.97 (d, *J* = 12.5 Hz, 1H), 3.83 (dm, J_{CH} = 140.4 Hz, 1H), 2.84 (dm, J_{CH} = 142.8 Hz, 2H), 1.66 (dm, J_{CH} = 128.4 Hz, 1H), 1.53 (dm, J_{CH} = 131.4 Hz, 3H), 1.28 (dm, J_{CH} = 132.6 Hz, 2H); **^{13}C-NMR** (D_2O, 151 MHz) δ 179.8 (d, *J* = 8.4 Hz), 179.5 (d, *J* = 8.4 Hz), 128.7 (s), 128.2 (s), 127.6 (s), 66.8 (s), 56.2 (ddd, *J* = 138.0, 46.2, 14.4 Hz), 55.8 (ddd, *J* = 139.2, 46.8, 15.0 Hz), 34.2 (dt, *J* = 161.0, 18.6 Hz), 31.1 (td, *J* = 138.6, 18.0 Hz), 23.2 (td, *J* = 138.6, 18.8 Hz), 22.0 (t, *J* = 137.4 Hz); $[\alpha]_D^{19}$:$-12.50 \pm 0.04^{\circ}$ (c = 2.00, 0.2 N HCl); **FTIR** (solid, cm^{-1}) 3306, 3031, 2931, 1717, 1654, 1497, 1402, 1369, 1344, 1232; **ESI-HRMS** (*m/z*): calcd for $C_8\,^{13}C_6H_{21}\,^{15}N_2O_4$ $(M+H)^+$ 289.1643, found 289.1650.

Supplementary Discussion

There are several features of the CTAP system that collectively distinguish it from other cell-selective protein labeling approaches. First, the products of enzymatic catalysis are canonical amino acids, allowing mature proteins to maintain their normal structure and avoiding functional alterations that may occur with methods based on amino acid analogs. Second, CTAP allows individual cell populations to be continuously labeled as they are grown and passaged over extended periods of time. Third, the genetic requirement of enzyme activity to overcome essential amino acid auxotrophy makes labeling controllable by limiting transgenic expression. Fourth, utilizing multiple enzyme-precursor pairs permits differential labeling of multiple distinct cell types during co-culture. Fifth, CTAP can be used to distinguish proteins from different cell types of the same organism rather than relying on artificial inter-species experimental setups. Finally, CTAP makes use of the same previously developed data-analysis workflows as the widely used SILAC method.

Three potential optimization steps could involve improving enzyme efficacy, decreasing enzyme secretion, or increasing precursor uptake. For example, we observed that *A. thaliana* DDC is more effective at rescuing growth than *E. coli* DDC (data not shown), suggesting that screening additional organisms or mutagenesis approaches may lead to more effective enzymes. Additionally, Saqib and collegues suggest that import of DAP is the primary limiting factor for production of L-lysine[3], and therefore future studies aimed at optimizing precursor import could further increase the efficiency of L-lysine production. While our attempts to rescue L-lysine auxotrophy with DDC and DAP have been successful in all cells tested, another group has reported variable rescue efficiency of *E. coli* DDC across cell types[4]. Although growth rescue was achieved in five cell lines representing distinct lineages, it remains to be seen whether the enzyme-precursor pairs presented here can be applied to all vertebrate cells.

References

[1] Cox, J. & Mann, M. MaxQuant enables high peptide identification rates, individualized p.p.b.-range mass accuracies and proteome-wide protein quantification. *Nat Biotechnol* **26**, 1367–72 (2008).

[2] Cox, J. *et al.* Andromeda: a peptide search engine integrated into the MaxQuant environment. *J Proteome Res* **10**, 1794–805 (2011).

[3] Saqib, K. M., Hay, S. M. & Rees, W. D. The expression of Escherichia coli diaminopimelate decarboxylase in mouse 3T3 cells. *Biochim Biophys Acta* **1219**, 398–404 (1994).

[4] Jouanneau, J., Stragier, P., Bouvier, J., Patte, J. C. & Yaniv, M. Expression in mammalian cells of the diaminopimelic acid decarboxylase of Escherichia coli permits cell growth in lysine-free medium. *Eur J Biochem* **146**, 173–8 (1985).